CSIRO PUBLISHING

International Journal of Wildland Fire
http://dx.doi.org/10.1071/WF11020

A mathematical model for predicting the maximum potential spotting distance from a crown fire

Frank A. Albini[A,F], *Martin E. Alexander*[B,C,E] *and Miguel G. Cruz*[D]

[A]Montana State University, Department of Mechanical and Industrial Engineering, Bozeman, MT 59717-3800, USA.
[B]Canadian Forest Service, Northern Forestry Centre, 5320-122 Street, Edmonton, AB, T6H 3S5, Canada.
[C]Present address: University of Alberta, Department of Renewable Resources and Alberta School of Forest Science and Management, Edmonton, AB, T6G 2H1, Canada.
[D]Bushfire Dynamics and Applications, CSIRO Ecosystem Sciences and Climate Adaptation Flagship, GPO Box 1700, Canberra, ACT 2601, Australia.
[E]Corresponding author. Email: mea2@telus.net
[F]Deceased 3 December 2005.

Abstract. A mathematical model is presented for predicting the maximum potential spot fire distance from an active crown fire. This distance can be estimated from the height of the flame above the canopy top, wind speed at canopy-top height and final firebrand size (i.e. its residual size on alighting), represented by the diameter of a cylinder of woody char. The complete model system comprises several submodels or components: a model for the height and tilt angle of the wind-blown line-fire flame front, a simplified two-dimensional model of the wind-blown buoyant plume from the fire, an assumed logarithmic wind speed variation with height, and an empirically based model for the burning rate of a wooden cylinder in cross flow, which represents the firebrand. The trajectory of the burning particle is expressed analytically from where it leaves the lower boundary of the plume until it enters the canopy top. Adding the horizontal distance of this flight to that of the point where the particle can no longer be held aloft by the plume flow gives a spotting range that depends on the final diameter of the burning particle. Comparisons of model output with existing information on crown fire spotting distances has initially proved encouraging but further evaluation is warranted.

Additional keywords: canopy-top height, crowning, ember, extreme fire behaviour, fire plume, firebrand, flame height, ignition, spot fire, wind speed.

Received 3 February 2011, accepted 6 December 2011, published online 18 June 2012

Introduction

Spotting is a common phenomenon associated with crown fires in conifer forests and can, in certain circumstances, be an important mechanism determining their overall spread (Rothermel 1983; Alexander and Cruz 2006). Estimation of the maximum distance at which a particular fire can spawn new fires by wind-borne burning embers often arises in planning wildland fire suppression operations or prescribed burning activities (Alexander 2000; Weir 2009). Experimental and theoretical work on the general topic of spotting in wildland fires has appeared in print sporadically for many years (e.g. Tarifa *et al.* 1965; Cheney and Bary 1969; Lee and Hellman 1970; Grishin *et al.* 1981; Ellis 2011), as have periodic reviews (e.g. Babrauskas 2003; Pastor *et al.* 2003; Koo *et al.* 2010).

Simplified models for estimating this distance have been created for specific situations, including the 'torching' of individual trees or small groups of trees (Albini 1979), burning piles of slash or 'jackpots' of heavy fuels[A] (Albini 1981*a*), and wind-aided surface fires in non-tree canopied fuel complexes such as grass, shrubs and logging slash (Albini 1983*a*, 1983*b*; Morris 1987). All of these models have found their way into operational use in various forms over the years (Rothermel 1983; Chase 1981, 1984; Finney 2004; Andrews *et al.* 2008). None of them were considered applicable to situations involving severe fire behaviour such as crown fires and firewhirls (Albini 1983*a*; Chase 1984). Venkatesh *et al.* (2000) did however extend Albini's (1979) model to predict the maximum spotting distance from an active crown fire – i.e. a free-burning fire

[A]Beginning in the late 1980s, some wildland fire behaviour analysts or specialists began applying the Albini (1981*a*) maximum spot fire distance model from burning piles to burning structures in the wildland–urban interface (J. K. Steele, Confederated Salish and Kootenai Tribes Division of Fire, pers. comm., 2011).

characterised by the quasi-steady advancement of a tall and deep coherent flame front extending from the ground surface in a conifer forest to above the top of the canopy fuel layer. The result was a 20 to 25% increase in spotting distance. However, no mention was made of model predictions *v.* existing observations.

More recently, several studies applied physical-based models to the problem of firebrand transport and combustion (Koo *et al.* 2007; Sardoy *et al.* 2007, 2008; Wang 2011). These models solve a set of equations describing the conservation of mass, momentum, energy and species; some authors (e.g. Linn *et al.* 2002; Mell *et al.* 2007) claim that by their apparent completeness, these physical-based models should be able to predict most fire behaviour phenomena and their interaction with small-scale meteorological conditions. However, the computational demands of these physical-based models limit their application as predictive tools for operational purposes. As an example, Sardoy *et al.* (2007) point out that a typical run in a $1000 \times 400 \times 500$ m (x, y, z) domain takes ~100 h of CPU time on a 3-GHz processor. A simulation of FIRETEC on a $320 \times 320 \times 615$-m domain took 1 to 2 min per second of simulation time in a 64-processor supercomputer (Colman and Linn 2007). A typical modelling exercise of 150 to 200 s would take 3.3 to 6.7 h to run (Sullivan 2009; Clark *et al.* 2010).

When considering maximum spotting distances, the computational requirements of these physical-based models somewhat limit the analysis of their outputs. Observations from wildfires suggest that spotting distances between 1 and 2 km are common in high-intensity crown fires in conifer forests (Wade and Ward 1973; Kiil *et al.* 1977; Luke and McArthur 1978; Alexandrian 2002; Cruz and Plucinski 2007), although higher distances have been reported. The extension of Sardoy *et al.* (2007) and Koo *et al.* (2007) computational domains to encapsulate a realistic simulation approach would further escalate the CPU time requirements to replicate observations from wildfires.

The creation of a model for predicting the maximum spotting distance from a running or active crown fire suitable for operational use has been a long-awaited development in the field of wildland fire behaviour forecasting (Rothermel 1991). In the present study, we propose a simplified physical-based description of the main processes controlling spotting phenomena as applied to crown fires in conifer forests. This formulation depart from the models developed earlier on to predict maximum spotting distances for a torching tree or trees (Albini 1979, 1981*a*) and spreading surface fires in non-forested fuel types (Albini 1983*a*, 1983*b*). The submodels for flame structure, strength of the heat source and buoyant plume structure present a sounder physical treatment of the processes they aim to describe than the earlier models. This is expected to lead to improvements in the predictive capacity of the overall model system.

This paper focuses on burning embers that fall from what is essentially a two-dimensional (line-source) strongly buoyant plume bent over by the wind aiding the propagation of a fully developed crown fire with a fireline intensity (Byram 1959) typically greater than 4000 kW m^{-1} (Van Wagner 1977; Cruz *et al.* 2008; Alexander and Cruz 2011*b*). Specifically, the active crown fire in Van Wagner's (1977) classification scheme is addressed. The passive crown fire can probably be considered, for the purpose of estimating spotting distances, to be a sequence of isolated events of torching of individual trees or groups of trees (Albini 1979) in open conifer forest stands.

Spotting associated with fire whirls or any other unusual fire-induced phenomenology is also not considered here (Berlad and Lee 1968; Lee 1972). It is furthermore presumed that the fuel complex in which a crown fire is burning is a conifer forest type of some sort. The mathematical model presented here would therefore not be appropriate for the prediction of spotting distances in Australia's eucalypt forests as a result of the unique characteristics of the bark as a firebrand source (McArthur 1967; Luke and McArthur 1978; Ellis 2000; Gould *et al.* 2007). Spot fires at distances of up to 30 km or more have been reported ahead of the main advancing fire front in such fuel complexes (McArthur 1967; Cheney and Bary 1969).

This paper consists of seven parts. It begins with a conceptualisation overview of the mathematical model and its associated simplifying assumptions. Next, the two primary modules or components of the model are described in detail (i.e. wind-blown plume from a line fire and firebrand trajectories). The shape and strength of the wind-blown plume are then graphically depicted, followed by a description of the firebrand trajectories in relation to the logarithmic wind-speed profile. Sample calculations from the mathematical model are then presented. The paper closes with a discussion of the limitations associated with the model and the difficulty of comparing model predictions with observational evidence.

Certain sections of the paper are by necessity highly mathematical in nature. For the convenience of the reader, a summary list of the variables referred to in the equations and text, including their symbols and units, is given at the end of this article.

Conceptualisation and simplifying assumptions in the mathematical model

Chandler *et al.* (1983, p. 104) very succinctly outline the spotting phenomenon involved in wildland fires:

> A firebrand or burning ember is lofted into the rising stream of flame and combustion gases, rises in the convection column until it is ejected into the ambient wind field, and falls under the influence of gravity while being moved laterally by the wind until it lands on the surface. If the firebrand has sufficient energy left when it lands, a spot fire will result.

The mathematical model for predicting the maximum potential spotting distance from an active crown fire as considered in the present paper directly addresses all of these individual processes except for the last one.

The three-dimensional convection column that arises from the consolidation of the heated air and products of combustion from a large burning area has been treated by Morton (1965). This structure, which can extend to the tropopause in the case of a large fire of high heat-release rate (Fromm and Servranckx 2003), often deposits downwind large amounts of ash and small charred fuel fragments (Anderson 1968; Pisaric 2002; Tinner *et al.* 2006), but seldom is reported as the source of long-range spot fires. This is probably because any embers that are burning

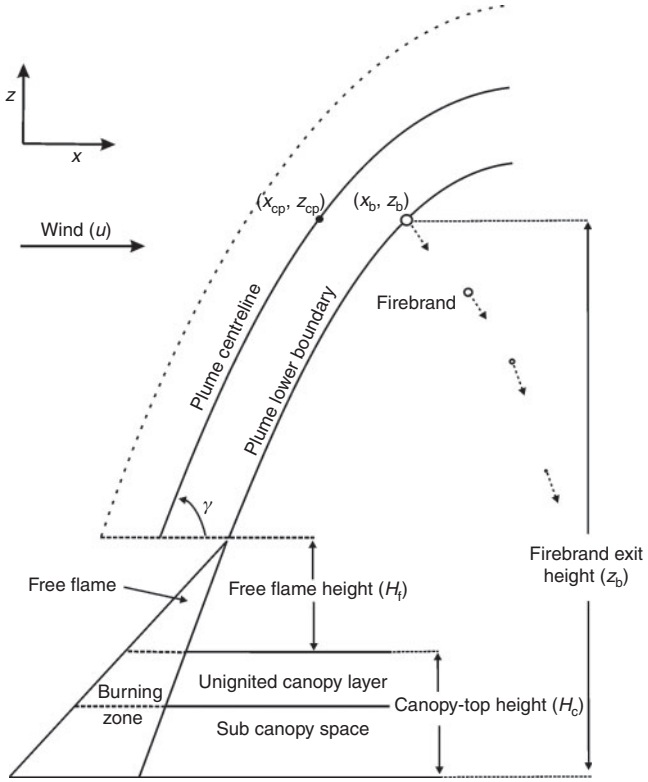

Fig. 1. Schematic diagram depicting the conceptualisation of the mathematical model for predicting the maximum potential spotting distance from an active crown fire in a conifer forest.

while being transported by the wind are consumed completely before returning to the surface. To travel far downwind of its heat source, a firebrand particle must first be raised to a great height (Albini 1979), but when a viable firebrand falls, its survival to the surface is determined by its height and size as it begins its descent.

For the purpose of estimating the greatest distance at which an active crown fire can be expected to spawn spot fires, the following conceptualisation (Fig. 1) of the flow field is analysed: a wind-aided line fire is the source of a two-dimensional buoyant plume that creates a region of stagnant air near the lee edge of the fire front (Rothermel 1993; Clements *et al.* 2007; Butler 2010). A line-fire plume was also assumed in the Albini (1983*a*, 1983*b*) surface fire spotting model. This is in contrast to the torching tree and pile-burning spotting models of Albini (1979, 1981*a*) that assume a self-similar, radially symmetrical turbulent buoyant plume.

From the flanks of the fire, the ambient wind field encroaches towards the centre of the fire front, eroding the stagnant air region. If the line fire is sufficiently long, there will occur 'breaks' and irregularities in the fire front (Grishin 1997) that allow the ambient wind field to penetrate the curtain of the plume, bringing horizontal momentum to the nominally stagnant region. Further downwind of the main advancing fire front, the ambient wind field once again regains its previous strength, modified by the presence of a plume flow imbedded within it.

The early stage of the plume flow is of interest here. It is modelled in simplified form by treating it as a uniform flow arising from the thorough mixing of the ambient wind field with a hot air stream issuing from a slot source at the tip of the flame. The lee side of the flow is considered to be stagnant, but entrainment into the plume from that side is ignored for simplicity's sake on the grounds that the plume flow quickly achieves a horizontal velocity that is almost the same as that of the ambient wind field. This flow is presumed to include cylindrical particles of burning woody char (Albini 1979), even though it is fully recognised that other forest firebrand particles such as bark flakes and cone scales, for example, exist (Clements 1977; Almeida *et al.* 2011). They are transported at local horizontal speed while falling at terminal relative velocity. At the point where plume vertical velocity equals particle terminal velocity, they fall from the plume. It is further assumed that they emerge into the ambient wind field, by which they are carried horizontally while falling at terminal velocities. This distorted model of the wind field is used to estimate the maximum spotting distance to be expected. Other than these simplifying assumptions, no further fire–atmosphere interactions such as discussed by Bhutia *et al.* (2009), for example, are considered.

All the of the maximum spotting distance models developed by Albini (1979, 1981*a*, 1983*a*), including the present one, are for flat terrain and must be corrected for use in mountainous terrain (see Chase 1981, p. 16). In cases where any of the models are implemented within a geographic information system (GIS)-based fire-growth simulator such as FARSITE (Finney 2004), there is no need for the correction as the simulator tracks the particle's (x, y, z) coordinates, in which case a firebrand is assumed to alight when its coordinates are equal to the surface (x, y, z) coordinates.

As with the previous models developed by Albini (1979, 1981*a*, 1983*a*) for predicting the maximum spotting distances for various wildland fire situations, there are several factors that are omitted from the model presented here. These include (after Albini 1979):

(1) The likelihood of a crown fire occurring. No consideration is included here of the probability of crowning. The model must be thought of as a 'what if' decision aid and thus the user must gauge whether a crown fire is possible by whatever means are available to him (e.g. Taylor *et al.* 1997; Finney 2004; Alexander *et al.* 2006; Andrews *et al.* 2008; Cruz *et al.* 2008).
(2) Availability of optimum firebrand material. The model presumes that at least one ideally suited firebrand particle exists. This is consistent with the intent to estimate the maximum potential spotting distance.
(3) Probability of spot fire ignition. For a spot fire to start, the firebrand must come into contact with easily ignited dry fuel. The model does not deal with the chance of such contact or the probability that ignition will occur if contact is made; some experimental work has been undertaken on this latter point (e.g. Blackmarr 1972; Weir 2004; Beverly and Wotton 2007). The model predicts the maximum distance that a firebrand can travel and still retain the possibility of starting a spot fire.
(4) The number of spot fires. In keeping with the prediction of the maximum potential spotting distance, neither the spot

fire density (i.e. number of spot fire ignitions per unit surface area) nor spot fire ignition probability are considered in the model as described here. Such determinations must be made other means (e.g. Hirsch *et al.* 1979).

Model development: the wind-blown plume from a line fire

Under the assumptions described above, the initial part of the two-dimensional buoyant plume from a line fire can be modelled readily. The model of the plume flow is first presented here, along with the ambient wind-field profile used in this analysis. The flame structure model, which allows inference of the intensity of the line fire from observation of its flame height, provides the boundary conditions for the plume flow. It can be inferred from a generalisation of the flame structure model on which flame-tip conditions are based that the integral of the ambient wind speed over the extent of the free flame (i.e. the vertical height of the flame measured from the tops of the trees) is proportional to the intensity or power per unit length of the fire. So the flame height can be used, along with the ambient wind speed, to infer Byram's (1959) fireline intensity.

Simplified line-fire plume model

There have been many investigations of the buoyant plume from a line source, with a variety of motivations. Rouse *et al.* (1952) and Roberts (1979*a*, 1979*b*) modelled Boussinesq plumes in quiescent surroundings. Lee and Emmons (1961) also modelled and measured such flows. Roberts (1980) extended his work to include the effect of ambient flow perpendicular to a line source. Gostintisev and Sukhanov (1977) modelled a wind-blown, strongly buoyant plume from a line fire in a uniform atmosphere and Gostintisev and Sukhanov (1978) did so in a polytropic atmosphere, including explicit turbulence models. The latter works, for example, are some of the most sophisticated by far, and would form a cogent basis for a spotting-distance model of high fidelity. But respecting the principle that a series of computations can be no more precise than the least accurate of its components, it seems appropriate for this application to construct the simplest model that contains the basic phenomenology of the strongly buoyant wind-blown linear plume. The uncertainty of spotting distance introduced by the gross nature of the plume structure model is thought to be no greater than that due to the uncertainties introduced by the empirical models for flame structure and for the firebrand burning rate.

To this end, the two-dimensional line plume in a cross-wind is treated as marking a division between the ambient wind field and a mass of stagnant air. Air is presumed to be incorporated into the plume flow on its windward side but entrainment from the stagnant air on the leeward side is neglected. This model should retain the integrity of the plume flow to the maximum extent, presumably overestimating the capability of the plume to lift large firebrand particles to heights at which they might not survive the return fall to the surface. As such heights are no more than a few hundred metres above the top of the canopy layer, the atmosphere can be considered to be uniform (i.e. atmospheric pressure, density and temperature do not vary with height). The plume flow structure is treated as uniform, so the velocity and fluid properties vary with distance along the plume's centreline but not across it. Air is considered to be an ideal gas with constant specific heat capacities.

Using the conceptual model described above, conservation of mass, momentum and energy in the fully mixed uniform plume flow and the equation of state for the plume fluid are expressed by:

$$\text{mass flux in plume flow: } m = \rho b V \tag{1}$$

$$\text{conservation of mass: } \frac{\mathrm{d}}{\mathrm{d}z} m = \rho_\mathrm{a} u_\mathrm{a} \tag{2}$$

$$\text{horizontal momentum: } \frac{\mathrm{d}}{\mathrm{d}z} mu = \rho_\mathrm{a} u_\mathrm{a}^2 \tag{3}$$

$$\text{vertical momentum: } \frac{\mathrm{d}}{\mathrm{d}z} mw = (\rho_\mathrm{a} - \rho) g b \tag{4}$$

$$\text{energy (neglecting kinetic energy) } \frac{\mathrm{d}}{\mathrm{d}z} m C_\mathrm{p} (T - T_\mathrm{a}) = 0 \tag{5}$$

$$\text{ideal gas at constant pressure } \rho T = \rho_\mathrm{a} T_\mathrm{a} \tag{6}$$

where m, the plume mass flux; ρ, the mass density; b, the plume width; V, the plume flow velocity parallel to the plume centreline (Fig. 1); u, horizontal air velocity, w, vertical air velocity; g, acceleration of gravity; C_p, the specific heat capacity of air and T, temperature. Subscripts a and p are relative to ambient conditions and firebrand. The ambient wind-field structure used for the plume model (and for firebrand transport calculations) is the logarithmic variation of wind speed with height (Albini 1981*c*). Equating the mean ambient wind speed at canopy-top height (U_c) to the friction velocity divided by the von Karman constant (0.40), the zero-plane displacement to 0.64 times the canopy-top height, and the roughness length to 0.13 times the canopy-top height (H_c) (Albini and Baughman 1979) and simplifying the results gives the following simple approximation for the variation of ambient wind speed (u_a) with height above the canopy top (z):

$$u_\mathrm{a} = U_\mathrm{c} \ln\left(e + 2.94 e \frac{z}{H_\mathrm{c}}\right) \tag{7}$$

Using this form, Eqn 2 can be integrated to provide the plume mass flux as a function of height (z) with the mass flux at the top of the flame (m_f) as a parameter:

$$m = m_\mathrm{f} + 0.34 \rho_\mathrm{a} U_\mathrm{c} H_\mathrm{c} \left\{ \left(1 + 2.94 \frac{z}{H_\mathrm{c}}\right) \ln\left(1 + 2.94 \frac{\mathrm{z}}{H_\mathrm{c}}\right) - \left(1 + 2.94 \frac{H_\mathrm{f}}{H_\mathrm{c}}\right) \ln\left(1 + 2.94 \frac{H_\mathrm{f}}{H_\mathrm{c}}\right) \right\} \tag{8}$$

The mass flux at the flame tip (m_f) is evaluated from the fireline intensity, which is inferred from the wind speed and the flame height using the flame structure model described in the next section (see also Albini 1981*b*). This gives:

$$m_\mathrm{f} = 0.468 \rho_\mathrm{a} U_\mathrm{c} H_\mathrm{c} \left(1 + 2.94 \frac{H_\mathrm{f}}{H_\mathrm{c}}\right) \ln\left(1 + 2.94 \frac{H_\mathrm{f}}{H_\mathrm{c}}\right) \tag{9}$$

which is of the same form as Eqn 8. The mass flux into the plume flow from the wind field between the canopy-top height and the flame tip is the same as the expression in Eqn 9 except that the numerical coefficient is 0.34 instead of 0.468. This indicates that the mass flux into the base of the free flame at the height of the canopy top must be the difference between the two, equal to the expression in Eqn 9 with a numerical coefficient of $0.468 - 0.34 = 0.128$.

Eqn 5 indicates that the product of mass flux and temperature excess in the plume is constant with height, giving the temperature profile simply related to the flame-tip temperature (T_f). Using a flame-tip temperature of 500 K (Albini 1981*b*) and a nominal 300-K ambient temperature provides the final form:

$$\frac{T}{T_a} = 1 + \frac{m_f}{m}\left(\frac{T_f}{T_a} - 1\right) = 1 + \frac{2}{3}\frac{m_f}{m} \tag{10}$$

This equation, along with Eqns 6, 8 and 9, gives the mass density profile with height, allowing the numerical integration of Eqn 4 to provide the vertical velocity variation with height.

Eqn 3, the horizontal momentum equation, can be integrated explicitly to give the variation of horizontal velocity (u) with height, using the logarithmic wind-speed profile. The horizontal momentum flux (i.e. $m \times u$) can be evaluated by integrating Eqn 3, using the wind-speed profile, from the height of the top of the canopy layer to height z. The value of the horizontal momentum flux in the flame flow at the canopy-top height is bounded by assuming that the mass flux into the free flame structure has horizontal speed equal to the flame-tip value. This is a clear overestimate but is of little or no consequence, because this mass flux is only a fraction of the flame-tip value. The analytical simplification afforded by this approximation is preferred over any hypothetical increase in precision by using a lower horizontal velocity for this added mass flux:

$$\frac{mu}{\rho_a U_c^2 H_c} = \frac{z}{H_c} + 0.34\left(1 + 2.94\frac{z}{H_c}\right)\ln^2\left(1 + 2.94\frac{z}{H_c}\right) + 0.3765\left(\frac{H_f}{H_c} + 0.34\left(1 + 2.94\frac{H_f}{H_c}\right)\ln^2\left(1 + 2.94\frac{H_f}{H_c}\right)\right) \tag{11}$$

The first two terms on the right-hand side of this expression represent the horizontal momentum flux incorporated into the plume flow between the top of the canopy layer and the height z. The third term is the upper bound approximation for the horizontal momentum flux of the flame fluid flow at the height of the canopy top.

To close the relationships above and solve for the thickness of the plume, the velocities are combined to give the speed of the flow along the central plane direction and then the width or thickness of the plume flow (b) is determined from Eqn 1:

$$V = \sqrt{u^2 + w^2} \tag{12}$$

$$\frac{b}{H_c} = \frac{m}{\rho V H_c} \tag{13}$$

The simulation calculations begin with the assessment of conditions at the tip of the flame. Then, small steps are taken along the central plane of the plume flow from the top of the canopy (s), say $\Delta s = 0.1 H_c$ in length. At each step, the conditions of the plume flow are evaluated, as is the angle of inclination of the central plane (γ) and the location of the central plane (x_{cp}, z_{cp}):

$$\begin{aligned} \Delta x_{cp} &= \Delta s \cos\gamma \\ \Delta z_{cp} &= \Delta s \sin\gamma \\ \gamma &= \sin^{-1}\left(\frac{w}{V}\right) \end{aligned} \tag{14}$$

where x is the distance downwind from the fire front, s is the distance along the central plane of the plume. In this way, the locus of the central plane is determined, and so also the location of the lower boundary of the plume flow:

$$\begin{aligned} x_b &= x_{cp} + \tfrac{b}{2}\sin\gamma \\ z_b &= z_{cp} - \tfrac{b}{2}\cos\gamma \end{aligned} \tag{15}$$

The dimensionless dynamic pressure of the vertical component of the plume flow, q, which determines its ability to keep aloft potential firebrand particles, is tabulated during this calculation for later look-up:

$$\frac{q}{\rho_a U_c{}^2} = \frac{1}{2}\frac{\rho}{\rho_a}\left(\frac{w}{U_c}\right)^2 \tag{16}$$

Flame-tip conditions

Conditions at the tip of the flame provide the boundary conditions for the plume structure model. The basic relationships are generalisations extracted from a flame structure model (Albini 1981*b*) that has admittedly not yet been adequately tested. The intensity of the fire (I) reduced for irretrievably lost radiant energy (r) powers the convective flow into the buoyant plume (USDA Forest Service 1960). The fireline intensity is thus related to the mass flux and temperature excess of the flame-tip flow, and, by the flame structure model, to the mass accreted by the free flame:

$$m_f C_p (T_f - T_a) = (1 - r) I \tag{17}$$

$$\begin{aligned} AI &= \int_0^{H_f} u_a \mathrm{d}z = U_c \int_0^{H_f} \ln\left(e + 2.94 e \frac{z}{H_c}\right)\mathrm{d}z \\ &= 0.34 U_c H_c \left(1 + 2.94\frac{H_f}{H_c}\right)\ln\left(1 + 2.94\frac{H_f}{H_c}\right) \end{aligned} \tag{18}$$

with A being an empirical crown fire flame structure constant, currently taken as $2.65\ \mathrm{m^3\,MJ^{-1}}$ (Albini 1981*b*; Call 1997). Substituting for I from Eqn 18 into Eqn 17 provides an expression for the mass flux into the plume at the flame tip. Making use of the ideal gas relationships as follows ($k = 1.40$ for air):

$$P_a = \rho_a R T_a = \rho_a \frac{k-1}{k} C_p T_a \tag{19}$$

where P_a is pressure and R is the ideal gas constant. Considering a flame-tip temperature of 500 K (Albini 1981*b*), a nominal 300-K ambient temperature, a fraction of fireline intensity lost by radiation assumed to be 0.15 (Byram 1959), and an ambient pressure of 0.10 MPa, the above relationship can be written in dimensionless form as:

$$\frac{m_f}{\rho_a U_c H_c} = 0.468\left(1 + 2.94\frac{H_f}{H_c}\right)\ln\left(1 + 2.94\frac{H_f}{H_c}\right) \qquad (20)$$

The horizontal momentum flux incorporated into the flame structure between the canopy layer top and the flame tip is given by:

$$\Delta(mu) = \int_0^{H_f} \rho_a u_a^2 dz = \rho_a U_c^2 H_c \int_0^{\frac{H_f}{H_c}} \ln^2(e + 2.94ez)dz$$
$$= \rho_a U_c^2 H_c \left\{\frac{H_f}{H_c} + 0.34\left(1 + 2.94\frac{H_f}{H_c}\right)\ln^2\left(1 + 2.94\frac{H_f}{H_c}\right)\right\} \qquad (21)$$

To account for the horizontal momentum flux into the base of the flame, this expression is multiplied by the ratio of the mass flux at the flame tip to the mass flux added over the height of the free flame, to give the horizontal momentum flux at the tip of the flame:

$$\frac{m_f u_f}{\rho_a U_c^2 H_c} = \frac{0.468}{0.34}\left\{\frac{H_f}{H_c} + 0.34\left(1 + 2.94\frac{H_f}{H_c}\right)\ln^2\left(1 + 2.94\frac{H_f}{H_c}\right)\right\} \qquad (22)$$

The ratio of Eqn 22 to Eqn 20 provides the horizontal velocity of the flame fluid flow at its tip. The tilt angle of the free flame at its flame tip (the nominal streamline slope) is generalised from the approximate form given by Albini (1981*b*) for a constant wind speed:

$$ctn^2\gamma_f \approx \frac{3}{2}\overline{u_a^2}/gH_f = \frac{3U_c^2}{2gH_f^2}\int_0^{H_f} \ln^2\left(e + 2.94e\frac{z}{H_c}\right)dz \qquad (23)$$

or, simply by

$$ctn\gamma_f = 0.714\frac{U_c}{\sqrt{gH_c}}\frac{H_c}{H_f}$$
$$\left\{2.94\frac{H_f}{H_c} + \left(1 + 2.94\frac{H_f}{H_c}\right)\ln^2\left(1 + 2.94\frac{H_f}{H_c}\right)\right\}^{1/2} \qquad (24)$$

The tilt angle provides the vertical component of the velocity at the flame tip, as

$$\frac{w_f}{u_f} = \tan\gamma_f \qquad (25)$$

Finally, the mass average velocity of the fluid flow at the flame tip (V_f) can be calculated from its components. This permits evaluation of the width of the plume flow at the flame tip, b_f, as the mass density of the flame fluid there is simply T_a/T_f (or 0.6 from 300/500 K) times the ambient density, from the ideal gas law:

$$V_f = \sqrt{u_f^2 + w_f^2}$$
$$\frac{b_f}{H_c} = \frac{m_f}{\rho_f V_f H_c} = \frac{m_f}{0.6\rho_a V_f H_c} \qquad (26)$$

These equations provide the complete description of the plume at the flame tip, using as input information only the height of the free flame above the canopy-top height (H_f), the canopy-top height (H_c) and the wind speed at the canopy-top height (U_c). Dividing all lengths by the canopy-top height, mass density by ambient value and all velocities by $(gH_c)^{1/2}$ makes all variables, both input and output, dimensionless.

Model development: firebrand trajectories

Next, we consider the trajectories associated with a firebrand, both in-plume and out-of-plume. If a firebrand could be considered to be an inert object (i.e. if none of its properties changed with time), the modelling of its flight in the ambient wind field would be much simplified. But this is not the case, because to be a firebrand capable of potentially initiating a spot fire, the particle must be burning (i.e. glowing or smouldering) when it returns to the surface. A simple empirical model for the burning rate of a woody cylinder (Albini 1979) is used to represent the change in aerodynamic properties of a firebrand particle as it falls. The model for the motion of the firebrand rests on several assumptions, some of which are rigorously justifiable and one of which is the burning rate model, which should be buttressed by additional experimental investigation.

To represent a potential firebrand particle, a right circular cylinder of woody char is used. It is presumed to obey the following conditions:

(1) The particle orients itself within the plume in such a way as to present to the relative air speed its longitudinal aspect. This is the maximum drag condition for a cylinder of length/diameter ratio greater than one, and is aerodynamically the most stable orientation.
(2) The particle falls at terminal velocity. That is, the aerodynamic drag generated by its vertical motion is equal to its weight at all times.
(3) The horizontal velocity of the particle is everywhere the same as that of the mean wind speed. This assumption and the previous one are essentially the same, in that it can be shown that both conditions are achieved after a very short travel distance for particles of small diameter (a few millimetres) and low mass density, such as 100 kg m^{-3} typical of woody char (Sussot 1982; Himoto and Tanaka 2005).
(4) The rate of mass loss by the particle can be modelled as a rate of diameter reduction that is proportional to the relative wind speed or its falling velocity (Albini 1979).
(5) The firebrand particle is assumed to exit the plume at its lower boundary at the downwind location where its weight

can no longer be supported by the drag force created by the upward velocity and local mass density of the plume flow.

The trajectory of the unsupported particle that has exited the plume is described later.

The aerodynamic drag (F) on a right circular cylinder in cross-flow of air with mass density ρ is given by:

$$F = \frac{1}{2}\rho W^2 C_D L D \tag{27}$$

where W is the air velocity relative to the firebrand particle, and C_D, L and D are the firebrand particle drag coefficient, length and diameter. The drag coefficient for this case is ~1.2 over a large range of velocities, and can be taken to be constant (Albini 1979). If the particle is being borne along horizontally at the local wind speed, but falling at terminal velocity, the drag force is equal to the weight of the particle, so:

$$F = \frac{\pi}{4} D^2 L \rho_p g \tag{28}$$

This yields the terminal velocity expression:

$$W_t = \sqrt{\frac{\pi \rho_p g D}{2 C D \rho_a}} \tag{29}$$

where the ambient air density ρ_a has been used for ρ.

If the ambient wind speed is $u(z)$, a function of the height (z) of the particle above the crown tops, then the trajectory of the particle is determined by the coupled linear differential equations:

$$\begin{aligned} \frac{dx}{dt} &= u(z) \\ \frac{dz}{dt} &= w(z) - W_t \end{aligned} \tag{30}$$

The burning rate model, derived from dimensional considerations and experimental work (Albini 1979), is taken to be:

$$\frac{dD}{dt} = -K\frac{\rho_a}{\rho_p} W_t = K\frac{\rho_a}{\rho_p}\frac{dz}{dt} \tag{31}$$

where the dimensionless constant K is 0.0064 (Albini 1979) and the density ratio, considering charred wood, can be taken to be 0.01 without loss of generality. Using these values, the burning rate law translates into a diameter v. height relationship:

$$D = 6.4 \times 10^{-5} z + \text{constant} \tag{32}$$

If we denote by subscript b the diameter and height where the firebrand particle exits the lower boundary of the plume and by c the diameter at the height of top of the crown layer, then:

$$D = D_c + vz$$

so

$$D_b = D_c + vz_b \tag{33}$$

where v is the decrease of firebrand diameter per unit height change. $D_c \geq vH_c$ if the particle is to survive the fall from crown-top height to the surface. Inserting this dependence into Eqn 30, Eqn 30 into Eqn 31, and dividing dx/dt by dz/dt yields the equation for the particle trajectory:

$$\frac{dx}{dz} = -\frac{u(z)}{W_{tb}}\sqrt{\frac{D_c + vz_b}{D_c + vz}} = -\frac{U_c \ln(e + 2.94e^{\frac{z}{H_c}})}{W_{tb}}\sqrt{\frac{D_c + vz_b}{D_c + vz}} \tag{34}$$

where W_{tb} is the particle's terminal velocity at diameter D_b from Eqn 29. This equation can be integrated explicitly, most readily using the diameter of the particle as the transformed independent variable rather than the height z. The result is, after some manipulation:

$$\begin{aligned} v\frac{W_{tb}}{U_c}\Delta x = {} & D_b\left(1 + \ln\left(1 + 2.94\frac{z_b}{H_c}\right)\right) \\ & - \sqrt{D_c D_b} + \sqrt{D_b(D_c - \delta)} \\ & \left\{\ln\left(\frac{\sqrt{D_b} + \sqrt{(D_c - \delta)}}{\sqrt{D_b} - \sqrt{(D_c - \delta)}}\right) - \ln\left(\frac{\sqrt{D_c} + \sqrt{(D_c - \delta)}}{\sqrt{D_c} - \sqrt{(D_c - \delta)}}\right)\right\} \end{aligned} \tag{35}$$

with δ, the firebrand diameter reduction function being:

$$\delta = 0.34 v H_c \tag{36}$$

The initial height above the top of the crown layer is determined by the condition that the plume flow cannot produce enough drag on the particle to keep it from falling. Equating the expressions given by Eqns 27 and 28 provides the condition on the dynamic pressure of the plume vertical flow where the particle can no longer be supported:

$$q = \frac{1}{2}\rho w^2 = \frac{\pi \rho_p g D_b}{4 C_D} \tag{37}$$

The algorithm that calculates the maximum potential spotting distance proceeds from the diameter of the particle on alighting (D_0) an assigned value, and correcting this value for the diameter loss as the firebrand travels from the height of the top of the crown layer to compute D_c. Then the diameter at exit from the plume (D_b) is found by adding the diameter loss as the particle travels from the top of the crown layer to the exit point:

$$\begin{aligned} D_c &= D_0 + vH_c \\ D_b &= D_c + vz_b \end{aligned} \tag{38}$$

In a table look-up procedure, the plume profile is searched to find the height z_b that satisfies Eqn 37 with D_b computed from Eqn 38. The value of x_b corresponding to this condition is then added to the distance increment Δx from Eqn 35 to yield the entire maximum spotting distance.

The firebrand diameter loss on falling from the height of the crown top is vH_c so if D_c is normalised by this quantity and used

as a parameter, then the ratio of D_b to H_c is determined. Denoting the ratio D_c/vH_c by η, the drift distance equation (i.e. Eqn 35) can be cast in the dimensionless form:

$$\frac{\Delta x}{H_c}\frac{\sqrt{gH_c}}{U_c} = \left(\frac{2C_D}{v\pi}\frac{\rho_a}{\rho_p}\left(\frac{z_b}{H_c}+\eta\right)\right)^{\frac{1}{2}} F\left(\frac{z_b}{H_c};\eta\right) \tag{39}$$

where

$$F\left(\frac{z_b}{H_c};\eta\right) = 1+\ln\left(1+2.94\frac{z_b}{H_c}\right) - \sqrt{\frac{\eta}{\eta+\frac{z_b}{H_c}}} + \sqrt{\frac{\eta-0.34}{\eta+\frac{z_b}{H_c}}}G\left(\frac{z_b}{H_c};\eta\right) \tag{40}$$

and the function G, describing the effect of initial firebrand height on spotting distance, is given by the following:

$$G\left(\frac{z_b}{H_c};\eta\right) = \ln\left(\frac{\sqrt{\eta+\frac{z_b}{H_c}}+\sqrt{\eta-0.34}}{\sqrt{\eta+\frac{z_b}{H_c}}-\sqrt{\eta-0.34}}\right) - \ln\left(\frac{\sqrt{\eta}+\sqrt{\eta-0.34}}{\sqrt{\eta}-\sqrt{\eta-0.34}}\right) \tag{41}$$

Shape and strength of the wind-blown plume

Using the logarithmic wind-speed profile described earlier, the plume shapes shown in Fig. 2*a–c* were generated. Dimensionless variables are used in each figure. The heights and horizontal distances are normalised by the height of the top of the crown layer, as is the 'free flame height', which represents the flame that extends above the top of the canopy layer.

The wind speed at the height of the top of the canopy layer is also a parameter in Fig. 2*a–c*. This velocity is normalised by the square root of the product of the canopy-top height and the acceleration of gravity. This dimensionless parameter is called a Froude number, which quantifies the ratio of specific kinetic energy of a fluid flow to the specific potential energy required to rise over a vertical barrier of a given height.

The upper and lower bounds of the plume are shown in these figures, along with the central plane of the plume flow. The central plane's locus is predicted by the model, along with the thickness of the plume measured perpendicular to this plane. This gives rise to the artefact of the break in slope of the upper and lower boundary shape predictions at the tip of the flame. These boundary shapes could be made to be smooth by allowing the width of the flow to vary over the height of the flame, but this would be an artificial constraint for the sake of appearance. The height of the lower boundary as a function of distance downwind from the fire front is the key prediction for spotting distance.

Fig. 2*a* shows the plume shape for a dimensionless wind speed of 1.0 and a free flame height of 1.5 times the canopy-top height. That is, if the tree stand is 10 m tall, then the flame would stand 15 m above the tops of the trees. The wind speed at tree-top height over the forest would be $\sim 10\,m\,s^{-1}$, as the acceleration of gravity is $\sim 10\,m\,s^{-2}$, making the normalising velocity $\sim 10\,m\,s^{-1}$.

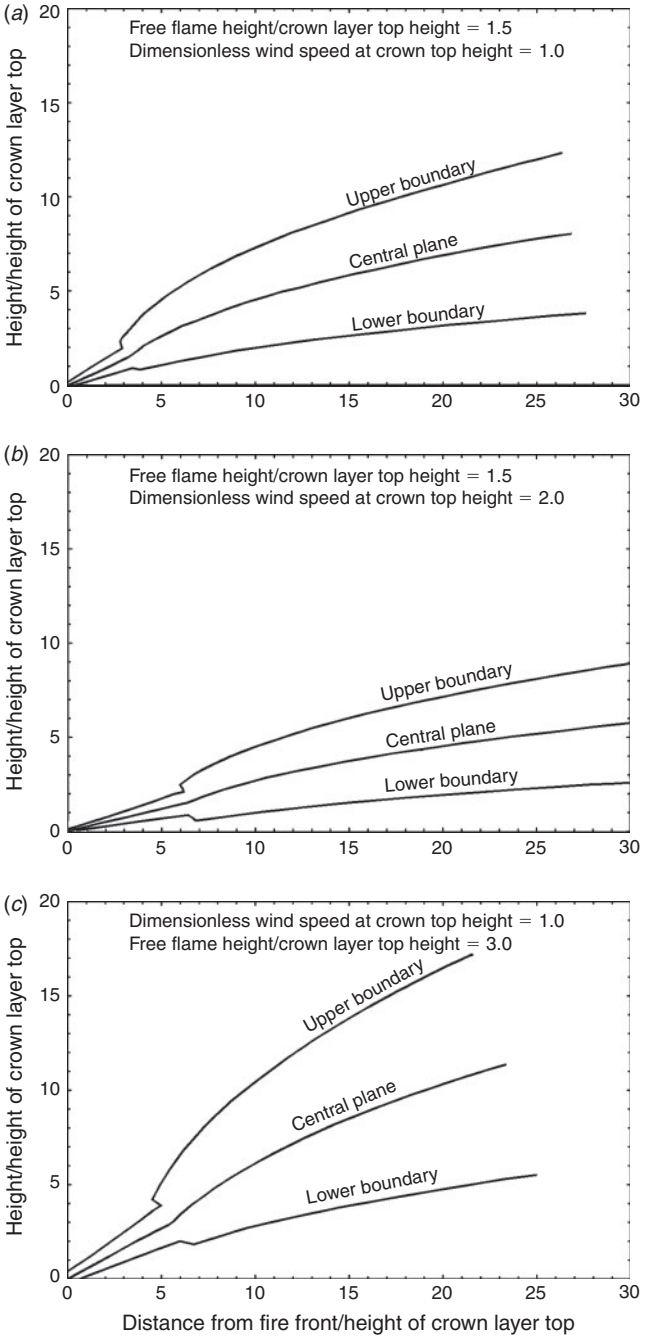

Fig. 2. Predicted shapes of the wind-blown plume near the front of active crown fires. Discontinuities in the upper and lower boundaries of the plume are an artefact of the crude method of starting the shape calculations, and represent no physical feature of the plume. The crown fire depicted in Fig. 2*b* has twice the intensity of the crown fire presented in Fig. 2*a* and twice the wind speed. The crown fire illustrated in Fig. 2*c* has the same wind speed as the crown fire presented in Fig. 2*a* and an intensity intermediate between the crown fires presented in Fig. 2*a* and 2*b*.

Fig. 2*b* shows the effect of doubling the wind speed while the flame height remains the same as in the previous case.

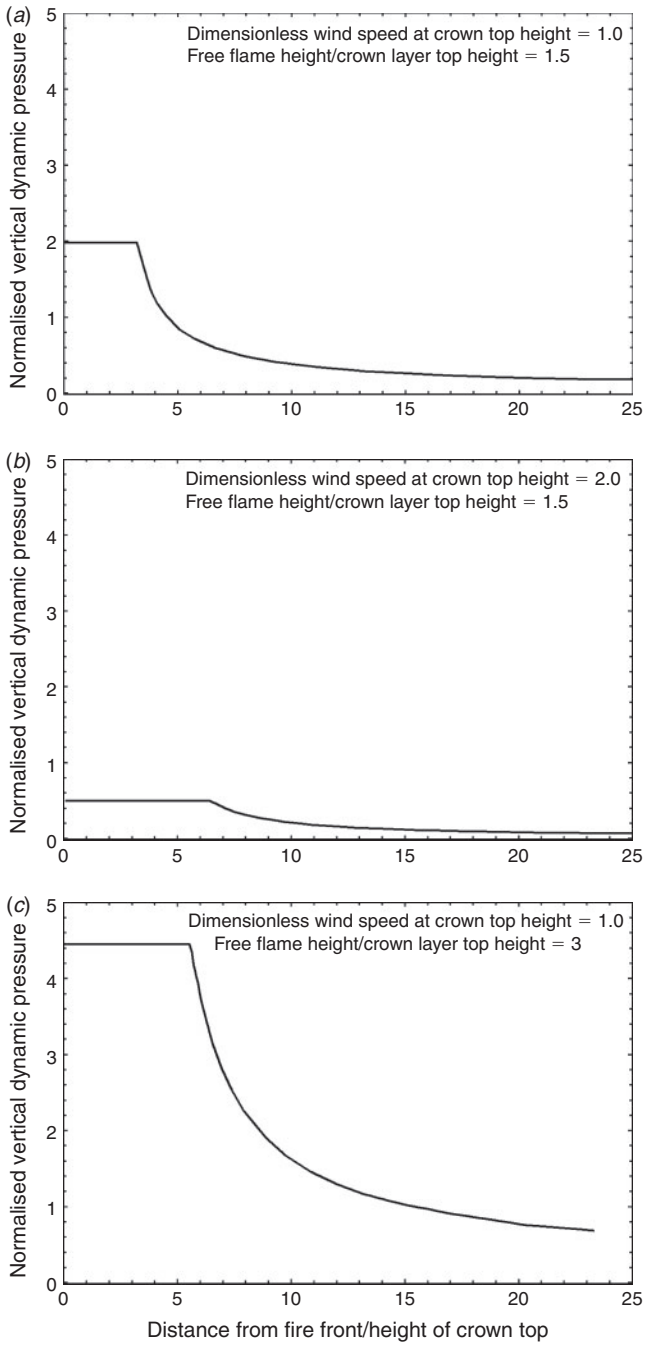

Fig. 3. Decay of firebrand lifting capability of the plume associated with the active crown fires presented in (*a*) Fig. 2*a*, (*b*) Fig. 2*b* and (*c*) Fig. 2*c*. The dynamic pressure is normalised by the product of ambient air density and the square of wind speed at the height of the top of the canopy layer. Only plume vertical velocity is used to compute the dynamic pressure.

The intensity of the crown fire has also doubled, according to the flame structure model, but the plume is elongated in the downwind direction. Fig. 2*c* shows the effect of doubling the flame height while the wind speed remains the same as in Fig. 1*a*. In this case, the intensity of the crown fire has increased, but is intermediate between Fig. 2*a* and 2*b*. The buoyant plume is substantially more erect in this case than in either of the other two.

The ability of the buoyant plume to transport firebrands is measured by the level of the dynamic pressure attributable to the vertical component of the plume fluid flow. The quantity called dynamic pressure is equal to the product of the mass density and the specific kinetic energy (or half the square of the velocity) of the fluid flow. In this case, only the vertical component of the velocity is important in holding firebrands aloft, so this is the quantity to be squared, not the entire velocity. Fig. 3*a* shows the decay of dynamic pressure with distance for the plume presented in Fig. 2*a*. The dynamic pressure is represented in dimensionless form, having been divided by the ambient air density and the square of the wind speed at the height of the top of the crown layer. Note that it decays quite abruptly after the tip of the flame and then declines much more slowly. In the first part of the plume, the flow is both bending over and slowing down, whereas in the later stages of plume development, the flow is almost horizontal and slowly declines in velocity as ambient air is incorporated into the plume. This incorporation cools the plume, raising the density of the fluid, so offsetting to some degree the effect of decreasing velocity. Fig. 3*b* and 3*c* illustrate the decay of vertical dynamic pressure for the plumes of Fig. 2*b* and 2*c* respectively. Note that there is ~1 order of magnitude difference in the vertical dynamic pressure levels of Fig. 3*b* and 3*c*. The plume presented in Figs 2*c* and 3*c* would be capable of lofting larger particles to greater heights than would the plumes depicted in Figs 2*b* and 3*b*.

Logarithmic wind-speed profile and firebrand trajectories

Equations for the path of the flight of a firebrand after it exits from the lower boundary of the plume were derived earlier on (i.e. Eqns 27–41). The basic assumptions are that the firebrand particle, assumed to be a circular cylinder of woody char, is carried horizontally at the local wind speed while it falls at terminal velocity. The terminal velocity changes as the diameter of the particle shrinks owing to burning, and the relationship between the particle diameter and the height through which it has fallen is a linear one.

The wind-speed profile through which the particle falls in this model is shown in Fig. 4. This is the logarithmic wind-speed profile usually associated with a constant shear stress layer in the atmospheric boundary layer. It is usually found over vegetation roughness when the atmosphere is dry and neutrally stable. This figure can be used to establish the wind speed at canopy-top height from measurements of wind speed above the canopy-top height. Below the canopy top, the mean wind speed usually exhibits an exponential profile with height (Albini 1981*c*).

To estimate the wind speed at canopy-top height from measurements in an opening but below that level (Crosby and Chandler 1966; Lawson and Armitage 2008), the logarithmic profile of Fig. 4 can be used. Replacing canopy-top height with vegetation cover height in the opening, extrapolate the wind speed to canopy-top height. This should provide a reasonable estimate if the measurement is made in a opening with adequate fetch. If the wind-speed measurement is made under the forest canopy, a reduction factor can be estimated based on the canopy layer density and figures given in Albini (1981*c*).

Fig. 5 shows the distance downwind that a burning firebrand particle will drift once it has left the plume. The downwind

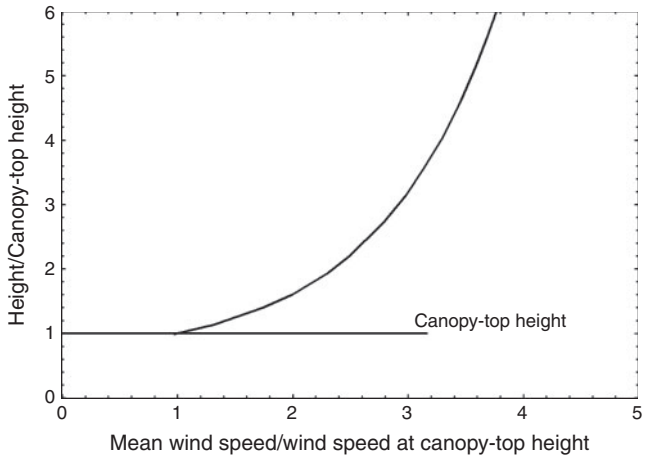

Fig. 4. The logarithmic wind-speed profile above the canopy-top height used for firebrand trajectories. This is the wind field through which the firebrand is presumed to fall, at continually changing terminal velocity, after it leaves the plume.

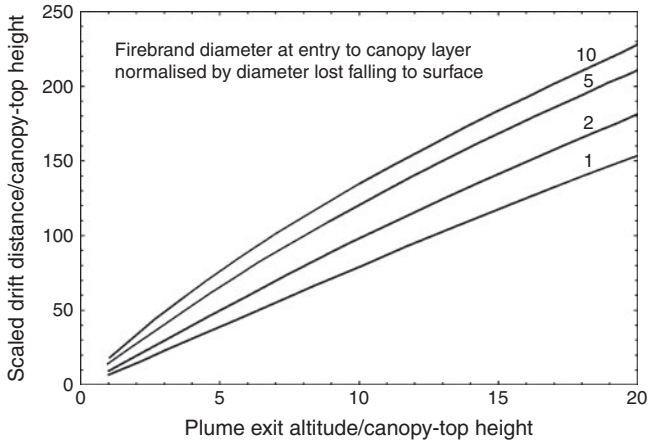

Fig. 5. Scaled, dimensionless firebrand downwind drift distance *v*. the height through which the firebrand falls after it exits the plume. The ratio of the firebrand's diameter on entering the canopy top to its diameter (mm) on alighting is the parameter associated with each curve. The uppermost curve is the case in which the firebrand loses its entire diameter by burning as it falls from canopy-top height to the surface.

distance is measured to the point where the firebrand particle enters the canopy top, rather than the point at which it presumably would alight. This is done for two reasons: (1) because the horizontal wind speed is much reduced below the canopy top, little additional drift would accrue, and (2) there is a high likelihood that a particle will mechanically encounter an obstacle within the canopy layer as it falls through, interrupting its downwind progress.

The downwind drift distance shown in Fig. 5 is scaled by the normalised wind speed at the canopy-top height. This is done for generality, because it allows the drift distance problem to be completely specified by using as a parameter the ratio of the diameter of the particle at the height of the top of the crown layer to its diameter on alighting. By this artifice, it is not necessary to specify explicitly the diameter of the firebrand when it alights.

Fig. 5 is not intended to be used for computational purposes, but rather to illustrate the sensitivity of firebrand drift distance to plume exit altitude, wind speed and diameter of the firebrand on alighting. For reference, a particle falling a distance of 15 m will lose ~1.0 mm of diameter. If it is presumed to alight with a diameter of 1.0 mm, then it would have to enter a 15-m canopy top with a diameter of 2.0 mm. The ratio of the diameter on entering the canopy to the diameter on alighting would be 2.0. Assuming that the particle fell from the plume 150 m above the canopy top, Fig. 5 would then be read at plume exit altitude ÷ canopy-top height = 10, revealing that the particle would have drifted ~115 canopy-top heights, or ~1.7 km if the normalised wind speed at canopy-top height were unity. That is, because the wind-speed normalising factor is the square root of the canopy-top height times the acceleration of gravity, or 12.1 m s^{-1}, Fig. 5 provides the information that if the wind speed at canopy-top height were 12.1 m s^{-1}, the firebrand drift distance would be 1.7 km. If the wind speed were doubled, the drift distance would be doubled; if the wind speed were halved, the drift distance would be halved.

Note that the uppermost curve of Fig. 5, for a diameter ratio of unity, gives the maximum possible spotting distance, because the firebrand particle will have been completely consumed at the instant of alighting. Using this limiting condition to estimate the maximum spot fire distance would be appropriate if one were not interested in 'prompt' spot fires, but in those that might emerge after some delay while smouldering in the organic mantle of the forest floor. Such smouldering fires can be ignited with very little total energy when it is concentrated in small, glowing embers (Thomas 1965, 1973). After some incubation period, they can burst into flame.

Sample calculations

Graphical representations of the output from the model system are presented here for three similar but different situations considered typical for active crown-fire conditions (Fig 6*a*–*c*). Each figure shows the estimated maximum potential spot fire distance (km) from the front of an active crown fire *v*. the diameter of the firebrand on alighting (mm) in relation to the canopy-top height (m), free flame height (m), and wind speed at the canopy-top height (m s^{-1}).

Fig. 6*a* is based on the following conditions: canopy-top height of 15 m, a free flame height of 22.5 m (so the distance from the surface to the tip of the flame would be 37.5 m) and wind speed at canopy-top height of 12.1 m s^{-1}. This crown fire is predicted to send 10-mm-diameter firebrands a distance of ~1 km ahead of the fire. Firebrands of such a size should be expected to start spot fires promptly on alighting. Firebrands of 1.0-mm diameter are predicted to land nearly 2.5 km ahead of the fire. Firebrands this small often will not immediately start spot fires, but they may initiate smouldering combustion in rotten wood or the forest floor layer (Burgan 1966; Stockstad 1979), to emerge as flaming fire starts after a variable period of delay. H. T. Gisborne gives a vivid account of one such incident that occurred on the 1926 Quartz Creek Fire (Gisborne 1927;

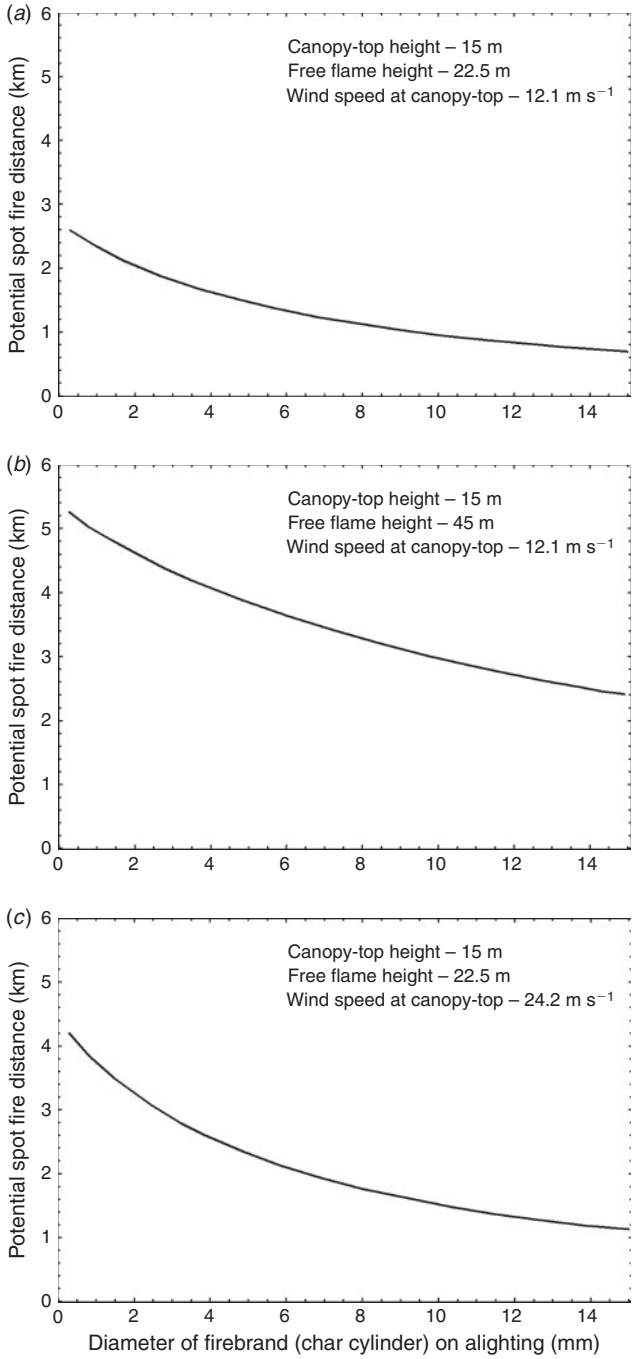

Fig. 6. Model prediction of the maximum spot fire distance from an active crown fire, as a function of the diameter of the firebrand (a charcoal cylinder) on alighting given (*a*) a free flame height of 22.5 m and a wind speed at the height of the canopy of 12.1 m s^{-1}; (*b*) a free flame height of 45 m and a wind speed at the height of the canopy of 12.1 m s^{-1} and (*c*) a flame height of 22.5 m and a wind speed at the height of the canopy of 24.2 m s^{-1}. A canopy-top height of 15 m is assumed in all three cases.

H. T. Gisborne, unpubl. data, 1934) in Kaniksu National Forest of northern Idaho, USA:

> In my experience on forest fires, I have actually seen only one case of a wind-blown ember falling and causing ignition. This was on the Quartz Creek fire on the Kaniksu in 1926, when a small twig, about one-eighth inch [~3-mm] diameter by one-half inch [~13 mm] long, fell from the smoke cloud above and came to rest on some rotten wood that I was looking at. As I examined the ember, without touching it, I saw that it was still glowing. During the four and a half minutes required to measure the temperature, humidity and wind, which were 78° [F; 25.6°C], 21% and 5.5 m.p.h. [8.9 km h^{-1}] respectively, this ember ignited the rotten wood, which ignited some dry grass and a minute or two later, this spot fire was crowning in a small Douglas-fir.

According to Albini (1979), the fact that an extremely small spark or ember can indeed ignite forest fuels has been established by experimental data (see also Ellis 2011).

The conditions specified in Fig. 6*b* show the effect of doubling the flame height compared with the situation presented in Fig. 6*a* but for the same given wind speed. In this case, the truly massive flames at the fire front reach 45 m above the tree tops, or 60 m from the surface, in spite of the high wind speed. This crown fire is predicted to send 10-mm-diameter firebrands ~3.0 km ahead of the fire front and 1.0-mm brands to ~5.0 km.

Fig. 6*c* shows the effect of doubling the wind speed compared with the situation presented in Fig. 6*a*. The extreme wind speed of 24.2 m s^{-1} at canopy-top height would bend the plume so severely that it would not be able to transport firebrands very high. Thus, despite the high wind speed, this crown fire is predicted to send 10-mm-diameter firebrands ~1.5 km, only 50% farther than the crown fire associated with Fig. 6*a*. Smaller-diameter particles, though, would spot farther in this case. The crown fire situation presented in Fig. 6*c* is predicted to send 1.0-mm-diameter firebrands 3.7 km ahead of the main fire front.

As shown in Table 1, the mathematical model is capable of producing maximum spot fire distances of upwards of 6 km for the highest ambient wind conditions likely to be experienced over land. In contrast, Albini's (1979, 1981*a*) single or group tree-torching model covers the case of intermediate-range spotting of up to perhaps ~1.5 to 3.0 km (Andrews and Chase 1989).

Comparison with other models

The present study concludes a fire behaviour modelling endeavour started in the late 1970s to develop mathematical models for predicting the maximum potential spotting distances associated with four distinct firebrand sources, namely individual or group-torching tree (Albini 1979, 1981*a*), surface fires in non-forested fuel types (Albini 1983*a*), burning debris piles (Albini 1981*a*), and now crown fires. Although there are some similarities among the four models, there are significant differences in the formulation of the models. These differences are a result of the particular configuration of each situation and the detail given to the physical description of the main processes involved.

To illustrate the differences between the models, we conducted a simulation of maximum spotting distance over level terrain (i.e. zero slope) as a function of 10-m open wind speed associated with five distinct fire-behaviour situations: (i) surface fire in grassland assuming the presence of woody firebrand material (Potter 2011); (ii) single-tree torching; (iii) torching of

Table 1. Maximum predicted spot fire distances on level terrain for an active crown fire as a function of average canopy-top height in relation to average height of flame above canopy top and the mean wind speed at canopy-top height

The two entries for free flame height for a given canopy-top height reflect the fact that the overall flame height is generally two to three times the height of a conifer forest stand (Alexander and Cruz 2011*b*). To convert the mean wind speed at canopy-top height to an estimate of the 10-m open wind speed, multiply by 1.5 (Lawson and Armitage 2008).The principal underlying assumption is that a 1.0-mm-diameter firebrand on alighting will result in an ignition. The conditions specified in this table bracket what would be considered a realistic range in free flame height, canopy-top height and wind speed at canopy-top height

Free flame height (m)	Wind speed at canopy-top height ($m\,s^{-1}$)					
	2.8	5.6	8.3	11.1	13.9	16.7
	Wind speed at canopy-top height ($km\,h^{-1}$)					
	10	20	30	40	50	60
			Canopy-top height – 5 m			
5	0.23	0.30	0.37	0.45	0.53	0.61
10	0.61	0.78	0.97	1.2	1.4	1.6
			Canopy-top height – 10 m			
10	0.52	0.64	0.78	0.92	1.1	1.2
20	1.2	1.5	1.8	2.2	2.5	2.8
			Canopy-top height – 15 m			
15	0.78	0.98	1.2	1.3	1.5	1.7
30	1.7	2.2	2.6	3.0	3.5	3.9
			Canopy-top height – 20 m			
20	1.1	1.3	1.5	1.7	1.9	2.2
40	2.1	2.9	3.4	3.9	4.4	4.9
			Canopy-top height – 25 m			
25	1.2	1.6	1.8	2.1	2.4	2.6
50	2.5	3.5	4.1	4.6	5.2	5.8

a large cluster or group of trees; (iv) pile of logging slash and finally (v) an active crown fire in a conifer forest. All of the maximum spotting distances were computed using *BehavePlus* (Andrews *et al.* 2008) except for the last situation.

The simulations involving the grassland and conifer forest fuel complexes were identical to those undertaken by Alexander and Cruz (2011*a*) in regards to simulating rate of fire spread, fireline intensity and flame depth. More specifically, the Cheney *et al.* (1998) natural pasture grass fuel type assuming a fuel load of $0.35\,kg\,m^{-2}$ and 100% degree of curing was used for rate of fire spread and in turn fireline intensity along with the flame length–fireline intensity relationship of Nelson (1980) as being more representative of grassland than Byram's (1959) relation (Alexander and Cruz 2012).

The following fuel-complex characteristics were employed in the Cruz *et al.* (2005, 2006) crown-fire initiation and rate of spread models for the conifer forest: available surface fuel load, $1.3\,kg\,m^{-2}$; canopy base height, 6.0 m; canopy fuel load, $1.8\,kg\,m^{-2}$; canopy bulk density, $0.23\,kg\,m^{-3}$; foliar moisture content, 100%; and stand height, 14 m. Crown-fire flame height in the conifer forest was estimated using the model of Butler *et al.* (2004). It is furthermore assumed that a 1.0-mm-diameter firebrand on alighting would result in an ignition.

The torching trees were red pine (*Pinus resinosa*) with a height and diameter-at-breast height of 14 m and 14 cm. A total of 30 trees were assigned to the group tree torching case. The downwind canopy height was assumed to be 14 m for both the single tree and the clump of trees. The threshold for torching is assumed to coincide with the onset of crowning. It is fully recognised that torching may in fact not occur under the influence of exceptionally strong winds.

A nominal slash pile height of 3.0 m was selected (G. J. Baxter, FPInnovations Wildland Fire Operations Research Group, pers. comm., 2011). In the absence of a flame-height model for burning slash piles, the continuous flame height input was judged to be, based on the work of Johansen (1981) and Johnson (1982), twice the pile or fuel height. Thus, a continuous flame height of 6.0 m is expected to be maintained, regardless of the strength of the wind conditions. It is fully recognised that flames greater than twice the pile height are quite possible (Johnson 1984).

An ambient air temperature of 30°C and a relative humidity of 20% was applied. This corresponds to a fine dead fuel moisture content of 6% for conifer forest (Rothermel 1983) and 4.8% for grass (Noble *et al.* 1980).

The results of the simulation as summarised in Fig. 7 highlight the relative differences in the maximum predicted spotting distances arising from several distinct firebrand sources for the same prevailing fire weather conditions. The data presented in Fig. 7 should be viewed as an approximation based on the assumed linkages between models for rate of fire spread, fireline intensity, flame-front dimensions and maximum spotting distances given that the choice of models can have a strong effect on the end result. Nevertheless, one can clearly see that the present model for crown fire predicts the longest maximum spotting distances of the models examined given the specified burning conditions.

It is worth comparing the results given in Fig. 7 for crown-fire spotting distances with the simulations performed by Sardoy *et al.* (2007, 2008) and Koo *et al.* (2007). Sardoy *et al.* (2007) modelled maximum spotting distances of 0.60–0.65 km for a non-spreading fire analogue with a fireline intensity of

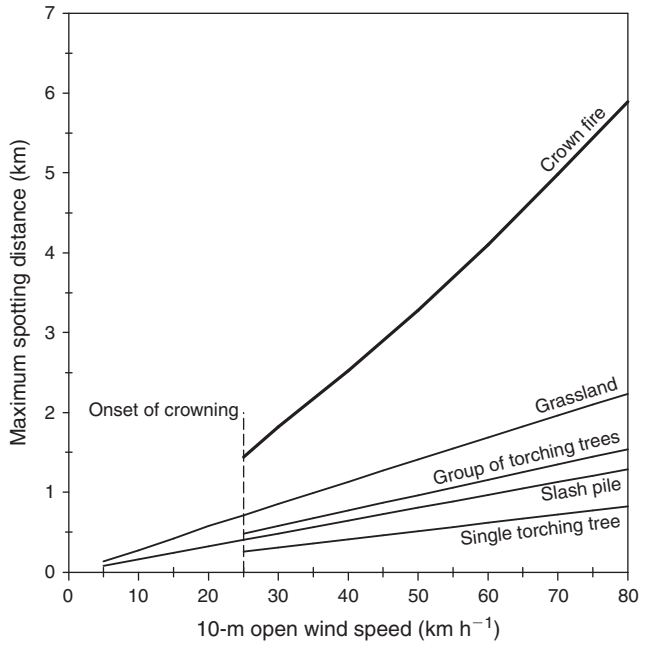

Fig. 7. Comparison of model predictions for maximum potential spotting distance over level terrain as a function of wind speed for a specified set of burning conditions. Refer to text for details on the fuel properties, fire behaviour characteristics and other weather parameters. A 10-m open wind speed >5 km h^{-1} is considered required for a consistently heading fire (Cheney *et al.* 1998).

40 000 kW m^{-1} and a fixed inlet wind speed (i.e. no vertical variation) of 24.1 km h^{-1}. In contrast, our simulation for a 10-m open wind speed of 25 km h^{-1} yields a fireline intensity of 21 800 kW m^{-1} and a maximum spotting distance of 1.4 km. The lack of any variation in wind speed with height might explain the shorter maximum spotting distances given in Sardoy *et al.* (2007). Sardoy *et al.* (2008) modelled ground-level distribution of firebrands under idealised fire intensities and wind speeds. Their modelling approach departs from Sardoy *et al.* (2007) by considering a simplified 2-D transport approach instead of 3-D. Sardoy *et al.* (2008) present detailed results for a simulation based on a fire driven by a fixed wind speed at canopy height of 40 km h^{-1} and an assumed intensity of 30 000 kW m^{-1}. Under these conditions, the model predicted maximum spotting distances of up to 9.5 to 10 km for the firebrands with highest char content.

Koo *et al.* (2007), however, simulated maximum spotting distances from a crown fire spreading at 70 m min^{-1} in a forest with an inlet wind speed of 21.6 km h^{-1} (no details on fuel moisture levels were given). Fireline intensity would have been comparable with the Sardoy *et al.* (2007) simulation. Simulations for two types of firebrands, discs and cylinders, were conducted, resulting in maximum spotting distances of 0.191 and 0.089 km; given these distances and the crown-fire rate of spread, any spot fires would be overrun in 2 to 3 min (Alexander and Cruz 2006). The maximum spotting distances associated with both the Koo *et al.* (2007) and Sardoy *et al.* (2007, 2008) simulations are obviously at variance with the predictions based on the model presented here.

Model predictions *v.* observational evidence

Model validation is considered part and parcel of continued model development (Jakeman *et al.* 2006). No validation data specifically collected for the purpose of directly testing the mathematical model as described in the present paper are currently available. Nevertheless, the estimates of the maximum potential spotting distances from active crown fires produced by the model appear to produce realistic predictions in light of documented observations made of long-range spotting associated with crowning wildfires in coniferous-dominated forests.

As mentioned in the introduction, spotting distances of up to ~2.0 km are commonly observed on crown fires in conifer forests (Partners in Protection 2003[B]; Beck and Simpson 2007; Forest Fire Management Group 2007). A few observations of spot fire distances of ~3.0 km have been made (USDA Forest Service 1952; Fryer and Johnson 1988) and spotting distances close to 5.0 km have been reported in the past in northern Idaho (Jemison 1932) and central Wisconsin (Haines and Smith 1987). Such a spot fire distance was also reported to have occurred during the 2003 fire season in British Columbia, Canada (D. S. Marek, British Columbia Wildfire Management Branch, pers. comm., 2010). Furthermore, Stocks (1995) explored the possibility that an ~7-km spot fire distance in north-central Ontario resulted from an escaped prescribed fire as opposed to a human-caused fire or a lightning-ignited holdover fire.

Brown and Davis (1973) claim that there are authenticated cases in the USA of spot fires set up to 11 km ahead of the main fire. Unfortunately, they give no specific details on the fuel types, topography or weather conditions involved with such occurrences. However, spotting distances of 6 to 10 km were reported to have occurred in the northern Rocky Mountains of the USA during the 1910 and 1934 fire seasons (Gisborne 1935; Koch 1978). The circumstances associated with the spotting distances of 16 to 19 km reported for the 1967 Sundance Fire in northern Idaho, USA (Anderson 1968; Rothermel 1968; Finklin 1973), as described by Berlad and Lee (1968) and Lee (1972), are undoubtedly beyond the predictive capacity of the mathematical model as described here. Spotting between 15 and 20 km was reported to have occurred in the radiata pine (*Pinus radiata*) plantation fuel types associated with the 1983 Mount Muirhead Fire in South Australia (Keeves and Douglas 1983; O'Connor and O'Connor 1993).

Admittedly, true spotting distances associated with active crown fires are difficult to ascertain given the uncertainties in the ignition delay, for example – i.e. the elapsed time between a firebrand alighting, subsequent ignition and the onset of fire spread (Alexander and Cruz 2006). This is just another example of the inherent difficulties in trying to unravel the complexities associated with spotting in wildland fires and attempts to

[B]The guidance given in Partners in Protection (2003, p. 5 of the Appendices) that 'Frequent spotting is possible up to 200 metres in advance of a crown fire (some embers drop as far as 2 kilometres ahead of the fire)' was provided by one of us (M. E. Alexander) based on personal experience and an extensive knowledge of the literature on the subject.

Table 2. The relative difficulty associated with validating the actual prevailing inputs and the output of the predictive system for estimating the maximum spotting distance from an active crown fire

Variable	Description of the issue(s) and possible solution(s)
Canopy-top height	Determining a value for this quantity can be easily accomplished from post-fire measurements or by visual estimation provided the general location or position of the main fire front that produced the spot fire can be determined with a reasonable degree of confidence. The more uniform the forested landscape, the less uncertainty that will be involved with this particular input variable.
Mean wind speed at canopy-top height	Provided it is possible to determine the times involved between lift-off and landing of the firebrand with a reasonable degree of accuracy, the greatest challenge in determining this value is the availability of representative weather stations and that the observations precisely match the relatively short flight time of the firebrand. Other means of gauging wind velocity (e.g. aircraft pilot estimates, ground observations using the Beaufort wind scale[A]), although useful, are generally not carried out in a systematic manner in order to derive a true estimate. Momentary gusts can easily occur, thereby complicating documentation matters.[C]
Free flame height[B]	The likelihood of observing the main head-fire flame front at the precise moment of firebrand lift-off would be exceedingly rare even given the subsequent discovery of a spot fire. However, observations made during the time of the general fire run coupled with a record of the head fire position at fairly frequent intervals and the corresponding canopy-top heights may enable a reasonable estimate to be deduced.
Maximum spotting distance	Although the discovery of a developing spot fire might by chance be made soon after the initiation of spread from the point of ignition, the opportunity for determining the firebrand diameter on alighting is likely near impossible. Given the spot fire size at discovery, it would be possible to estimate the elapsed time using a point-source fire growth model. Ascertaining the 'ignition delay'[D] is equally difficult, which makes it all the harder to determine the time and firebrand source location.

[A]List (1951).
[B]Byram (1959) indicated that efforts to objectively estimate flame heights of crown fires are complicated by the fact that 'sudden ignition of unburned bases in the convection column can result in flame flashes which momentarily extend several hundred feet [~100 to 200 m] into the convection column aloft'; Sutton (1984), for example, has photographically documented one such flame flash that extended almost 200 m above the ground over an exotic pine plantation in South Australia during the Ash Wednesday fires in 1983. According to Byram (1959) such flashes can easily result in overestimates of average flame heights 'which usually range from 50 to 150 feet [~15–45 m] on high-intensity fires'. Average flame heights are thus generally regarded as being approximately two to three times the canopy height (Alexander 1998).
[C]Crosby and Chandler (1966).
[D]Alexander and Cruz (2006).

validate a predictive system such as the present one, as described in Table 2.

In spite of technological advances in the ability for timely detection of spot fire activity, data suitable for validation or evaluation purposes are likely to accumulate slowly from the occasional 'windfall' observation, especially in the absence of a long-term, concerted effort devoted to wildfire monitoring and documentation (Alexander 2002). Consider for example that formal published documentation and performance feedback testing on Albini's (1979) maximum spot-fire distance model for torching trees is limited to the observations given by Norum (1982), Rothermel (1983) and Simard *et al.* (1983).

Following some 30 years of experience with the suite of Albini maximum spot fire distance models, operational users (e.g. wildland fire behaviour analysts or specialists) commonly point out 'that they generally never underpredict' (R. G. Lange-Navarro, USDA Forest Service, pers. comm., 2011). In this regard, the comments by Watts (1987, p. 93) seem very *a propos*:

> …if validation is a process for determining that the outputs of a model conform to reality, no model can be validated in an absolute sense; i.e. a model can never be proved correct, it can only be proven wrong. Acceptance of a model does not imply certainty, but rather a sufficient degree of belief to justify further action. Thus, in practice, validating a fire model is really a problem of invalidation. The more difficult it is to invalidate the model, the more confidence we have in it.

Taking into account the issues described in Table 2, the best prospects for obtaining data to validate or evaluate the performance of the predictive system for maximum spotting distance from active crown fires are cases that involve the breaching of major barriers to fire spread such as rivers and lakes (Alexander *et al.* 2004). These situations should be the focus of concentrated wildfire monitoring efforts as the opportunities present themselves (Alexander and Thomas 2003*a*, 2003*b*; Alexander and Taylor 2010).

Summary and concluding remarks

An idealised mathematical model for estimating the maximum spot fire distance from an active crown fire has been developed. The model rests on a set of assumptions, simplifications, approximations and empirical relationships detailed in this paper. Philosophically, these departures from exactitude are thought to be crudely in balance, in that no particular facet of the process of firebrand lofting, transport and consumption by burning dominates the error budget of the final distance estimate. In other words, the predictions are largely 'theoretical' at this stage. The present paper represents another contribution to the growing body of knowledge and work on the topic of spotting in wildland fires. Hopefully, through a more formal program of field observations and experimental testing (e.g. Colin *et al.* 2002; Rice *et al.* 2010), the more serious flaws in the prediction system can be identified and corrected through

continued research and development by the global wildland fire community as a whole.

The mathematical model described in this paper can be considered a hybrid or semiphysical model that integrates the robustness of first principles with simplifying empirical assumptions allowing the modelling of spotting phenomena as a closed system. The model as described herein builds on the previous modular approach to predicting maximum spotting distances from torching trees (Albini 1979) and spreading surface fires (Albini 1983*a*, 1983*b*), albeit the core components describing the heat source and buoyant plume dynamics depart considerably from these earlier efforts. The submodels for flame structure, strength of the heat source and buoyant plume have a sounder physical basis, which is expected to improve the overall predictive capacity. It is believed that the redesign of the earlier models developed by Albini (1979, 1983*a*) would inevitably benefit from incorporating some of the newer components described in this paper.

Model predictions are for the 'maximum' spotting distance because ideal conditions are assumed (Andrews and Chase 1989) rather than the average spotting distance (McArthur 1967). The mathematical model is thus likely to consistently overestimate spotting distances. For example, the maximum spotting distance of 1.6 km observed on the 2001 Chisholm Fire in central Alberta (Quintilio *et al.* 2001) occurred with wind gusts of 20.6 m s^{-1} (74 km h^{-1}).

Given the stochastic nature of the processes involved with the spotting phenomena in forest fires, the development of a model system that could yield probability distributions of spotting distances from active crown fires compared with the more simplistic deterministic prediction would constitute a worthy goal. However, such a capability makes validation of the core model all that more perplexing.

It is worth reiterating that the mathematical model presented here provides an estimate of the maximum potential spotting distance from active crown fire as a function of the firebrand particle diameter at alighting based simply on three inputs, namely, canopy-top height, free flame height (i.e. flame distance above the canopy-top height) and the wind speed at the height of the canopy. Other than firebrand size, no other physical or chemical characteristic is considered. As mentioned earlier, it does not address the question of whether a firebrand will actually cause a spot fire to occur – in other words, the probability of ignition (Manzello *et al.* 2006; Ganteaume *et al.* 2009). This aspect of assessing spotting potential must still rest on the use of existing guidelines (e.g. Lawson 1973; Roussopoulos 1978; Albini 1979; Rothermel 1983) coupled with case study information (Alexander and Thomas 2003*a*, 2003*b*; Alexander and Taylor 2010) and personal experiences (Gisborne 1948).

List of symbols, quantities and units used in equations and text

A, empirical crown-fire flame structure constant (estimated value = 2.65 m^3 MJ^{-1})
b, width of plume, measured perpendicular to its central plane (m)
C_D, drag coefficient of firebrand particle in cross-flow
C_p, specific heat capacity of air at constant pressure (kJ kg^{-1} K^{-1})
D, diameter of firebrand particle (m)
F, aerodynamic drag
g, acceleration due to gravity (9.81 m s^{-2})
H, height (m)
I, fireline intensity (kW m^{-1})
K, dimensionless constant (0.0064)
k, ratio of specific heat capacities for air (1.40)
L, length of firebrand particle (m)
m, plume mass flux, parallel to central plane (kg m^{-1} s^{-1})
P, pressure (Pa, N m^{-2})
q, dynamic pressure of upward flow in plume = $\frac{1}{2}\rho w^2$ (Pa, N m^{-2})
R, ideal gas constant (kJ kg^{-1} K^{-1})
r, fraction of fireline intensity irretrievably lost by radiation (estimated here to be a minimal 0.15)
s, distance along central plane of plume, from top of canopy layer (m)
T, temperature (K)
u, air horizontal velocity (m s^{-1})
U_c, mean ambient wind speed at top of crown layer, (m s^{-1})
V, plume flow velocity, parallel to central plane (m s^{-1})
W, air velocity relative to firebrand particle (terminal velocity) (m s^{-1})
w, air vertical velocity (m s^{-1})
x, distance downwind from fire front (m)
z, height above top of crown layer (m)

Subscripts

a, ambient
b, lower boundary of plume flow
c, crown top
f, tip of flame
cp, central plane of plume flow
p, firebrand particle
t, terminal (velocity of particle)
0, at the ground surface below canopy

Greek letters

Δ, difference or change in value
γ, angle of plume flow central plane above horizontal (radians)
δ, firebrand diameter reduction function
η, ratio of firebrand diameter at crown top height to diameter on alighting
ν, decrease of firebrand diameter per unit height change
ρ, mass density (kg m^{-3})

Acknowledgements

This paper is based in large part on a report prepared under contract by the senior author (F. A. Albini) and submitted to the Canadian Forest Service; the first junior author (M. E. Alexander) served as the scientific authority. The financial support of the governments of Alberta, British Columbia, Quebec, Yukon Territory, and in particular the Northwest Territories are acknowledged with appreciation; in this regard, the assistance of W. Bereska, J. A. Beck, F. Lefebvre and A. K. Beaver is duly acknowledged. Special thanks are also extended to R. A. Lanoville for his support of this project. V. Babrauskas and R. M. Nelson Jr thoughtfully critiqued early

drafts of this paper. The comments of the associate editor and three reviewers ultimately resulted in a much improved paper. This article is a contribution in part of Joint Fire Science Program Project JFSP 09-S-03-1.

References

Albini FA (1979). Spot fire distance from burning trees – a predictive model. USDA Forest Service, Intermountain Forest and Range Experiment Station, General Technical Report INT-56. (Ogden UT)

Albini FA (1981*a*) Spot fire distance from isolated sources – extensions of a predictive model. USDA Forest Service, Intermountain Forest and Range Experiment Station, Research Note INT-309. (Ogden UT)

Albini FA (1981*b*) A model for the wind-blown flame from a line fire. *Combustion and Flame* **43**, 155–174. doi:10.1016/0010-2180(81)90014-6

Albini FA (1981*c*) A phenomenological model for wind speed and shear stress profiles in vegetation cover layers. *Journal of Applied Meteorology* **20**, 1325–1335. doi:10.1175/1520-0450(1981)020<1325:APMFWS>2.0.CO;2

Albini FA (1983*a*) Potential spotting distance from wind-driven surface fires. USDA Forest Service, Intermountain Forest and Range Experiment Station, Research Paper INT-309. (Ogden UT)

Albini FA (1983*b*) Transport of firebrands by line thermals. *Combustion Science and Technology* **32**, 277–288. doi:10.1080/00102208308923662

Albini FA, Baughman RG (1979) Estimating wind speeds for predicting wildland fire behavior. USDA Forest Service, Intermountain Forest and Range Experiment Station, Research Paper INT-221. (Ogden UT)

Alexander ME (1998) Crown fire thresholds in exotic pine plantations of Australasia. PhD thesis, Australian National University, Canberra, ACT.

Alexander ME (2000) Fire behaviour as a factor in forest and rural fire suppression. Forest Research in association with New Zealand Fire Service Commission and National Rural Fire Authority, Forest Research Bulletin 197, Forest and Rural Fire Science and Technology Series Report 5. (Rotorua and Wellington, NZ)

Alexander ME (2002) The staff ride approach to wildland fire behavior and firefighter safety. *Fire Management Today* **62**(4), 25–30.

Alexander ME, Cruz MG (2006) Evaluating a model for predicting active crown fire rate of spread using wildfire observations. *Canadian Journal of Forest Research* **36**, 3015–3028. doi:10.1139/X06-174

Alexander ME, Cruz MG (2011*a*) What are the safety implications of crown fires? In 'Proceedings of the 11th International Wildland Fire Safety Summit', 4–8 April 2011, Missoula, MT. (Ed. RL Fox) (CD-ROM) (International Association of Wildland Fire: Missoula, MT)

Alexander ME, Cruz MG (2011*b*) Crown fire dynamics in conifer forests. In 'Synthesis of Knowledge of Extreme Fire Behavior: Volume 1 for Fire Managers'. USDA Forest Service, Pacific Northwest Research Station, General Technical Report PNW-GTR-854, pp. 107–142. (Portland, OR)

Alexander ME, Cruz MG (2012) Interdependencies between flame length and fireline intensity in predicting crown fire initiation and crown scorch height. *International Journal of Wildland Fire* **21**, 95–113. doi:10.1071/WF11001

Alexander ME, Taylor SW (2010) Wildland fire behavior case studies and the 1938 Honey Fire controversy. *Fire Management Today* **70**(1), 15–25.

Alexander ME, Thomas DA (2003*a*) Wildland fire behavior case studies and analyses: value, approaches, and practical uses. *Fire Management Today* **63**(3), 4–8.

Alexander ME, Thomas DA (2003*b*) Wildland fire behavior case studies and analyses: other examples, methods, reporting standards, and some practical advice. *Fire Management Today* **63**(4), 4–12.

Alexander ME, Tymstra C, Frederick KW (2004) Incorporating breaching and spotting considerations into *PROMETHEUS* – the Canadian wildland fire growth model. Foothills Model Forest, Chisholm/Dogrib Fire Research Initiative Quicknote 6. (Hinton, AB)

Alexander ME, Cruz MG, Lopes AMG (2006) *CFIS*: a software tool for simulating crown fire initiation and spread. In 'Proceedings of 5th International Conference on Forest Fire Research', 27–30 November 2006, Figueira da Foz, Portugal. (Ed. DX Viegas) (CD-ROM) (Elsevier BV: Amsterdam, the Netherlands)

Alexandrian D (2002) A probabilistic model for forecasting spot fires. In 'Forest Fire Research and Wildland Fire Safety'. (Ed. DX Viegas) (CD-ROM) (Elsevier BV: Amsterdam, the Netherlands)

Almeida M, Viegas DX, Miranda AI, Reva V (2011) Effect of particle orientation and of flow velocity on the combustibility of *Pinus pinaster* and *Eucalyptus globulus* firebrand material. *International Journal of Wildland Fire* **20**, 946–962. doi:10.1071/WF09080

Anderson HE (1968) Sundance Fire: an analysis of fire phenomena. USDA Forest Service, Intermountain Forest and Range Experiment Station, Research Paper INT-56. (Ogden, UT)

Andrews PL, Chase CH (1989) BEHAVE: fire behavior prediction and fuel modeling system – BURN subsystem, part 2. USDA Forest Service, Intermountain Research Station, General Technical Report INT-260. (Ogden, UT)

Andrews PL, Bevins CD, Seli RC (2008) BehavePlus fire modeling system, version 4.0: user's guide. USDA Forest Service, Rocky Mountain Research Station, General Technical Report RMRS-GTR-106WWW Revised. (Fort Collins, CO)

Babrauskas V (2003) 'Ignition Handbook: Principles and Applications to Fire Safety, Fire Investigation, Risk Management and Forensic Science.' (Fire Science Publishers: Issaquah, WA)

Beck J, Simpson B (2007) Wildfire threat analysis and the development of a fuel management strategy for British Columbia. In 'Proceedings of Wildfire 2007 – 4th International Wildland Fire Conference', 13–17 May 2007, Seville, Spain. (CD-ROM) (Ministry of Environment and Junta de Andalucia: Madrid and Seville, Spain)

Berlad AL, Lee S-L (1968) Long-range spotting. *Combustion and Flame* **12**, 172–174. doi:10.1016/0010-2180(68)90101-6

Beverly JL, Wotton BM (2007) Modelling the probability of sustained flaming: predictive value of fire weather index components compared with observations of site weather and fuel moisture conditions. *International Journal of Wildland Fire* **16**, 161–173. doi:10.1071/WF06072

Bhutia S, Jenkins MA, Sun R (2009) Comparison of firebrand propagation prediction by a plume model and a coupled fire–atmosphere large-eddy simulator. *Journal of Advances in Modeling Earth Systems* **2**(4), 1–15.

Blackmarr WH (1972) Moisture content influences ignitability of slash pine litter. USDA Forest Service, Southeastern Forest Experiment Station, Research Note SE-173. (Asheville, NC)

Brown AA, Davis KP (1973) 'Forest Fire: Control and Use.' 2nd edn (McGraw Hill: New York)

Burgan RE (1966) Ignition probability in ponderosa pine needles and decayed Douglas-fir wood. MSc thesis, University of Montana, Missoula.

Butler BW (2010) Characterization of convective heating in full-scale wildland fires. In 'Proceedings of 6th International Conference on Forest Fire Research', 15–18 November 2010, Coimbra, Portugal. (Ed. DX Viegas) (CD-ROM) (University of Coimbra: Coimbra, Portugal)

Butler BW, Finney MA, Andrews PL, Albini FA (2004) A radiation-driven model of crown fire spread. *Canadian Journal of Forest Research* **34**, 1588–1599. doi:10.1139/X04-074

Byram GM (1959) Combustion of forest fuels. In 'Forest Fire: Control and Use'. (Ed. KP Davis) pp. 61–89, 554–555. (McGraw-Hill: New York)

Call PT (1997) Run-time optimisation of radiation-driven crown fire model. MSc thesis, Montana State University, Bozeman.

Chandler C, Cheney P, Thomas P, Trabaud L, Williams D (1983) 'Fire in Forestry. Volume I: Forest Fire Behavior and Effects.' (Wiley: New York)

Chase CH (1981) Spot fire distance equations for pocket calculators. USDA Forest Service, Intermountain Forest and Range Experiment Station, Research Note INT-310. (Ogden UT)

Chase CH (1984) Spotting distances from wind-driven surface fires – extensions of equations for pocket calculators. USDA Forest Service, Intermountain Forest and Range Experiment Station, Research Note INT-346. (Ogden UT)

Cheney NP, Bary GAV (1969) The propagation of mass conflagrations in a standing eucalypt forest by the spotting process. In 'Collected Papers of Mass Fire Symposium', Vol. I. (Commonwealth of Australia, Defence Standards Laboratory: Melbourne)

Cheney NP, Gould JS, Catchpole WR (1998) Prediction of fire spread in grasslands. *International Journal of Wildland Fire* **8**, 1–13. doi:10.1071/WF9980001

Clark MM, Fletcher TH, Linn RR (2010) A sub-grid, mixture-fraction-based thermodynamic equilibrium model for gas phase combustion in FIRETEC: development and results. *International Journal of Wildland Fire* **19**, 202–212. doi:10.1071/WF07116

Clements HB (1977) Lift-off of forest firebrands. USDA Forest Service, Southeastern Forest Experiment Station, Research Paper SE-159. (Asheville, NC)

Clements CB, Zhong S, Goodrick S, Li J, Potter BE, Bian X, Heilman WE, Charney JJ, Perna R, Jang M, Lee D, Patel M, Street S, Aumann G (2007) Observing the dynamics of wildland grass fires: FireFlux – a field validation experiment. *Bulletin of the American Meteorological Society* **88**, 1369–1382. doi:10.1175/BAMS-88-9-1369

Colin PY, Lampin-Cabaret C, Delboulbe E, Coste N, Marcillat J, Pereira JC, Binggeli F, Gaulier A, Botelho H, Loureiro C, Loddo G, Ditana E, Guijarro M, Hernando C, Diez C, Martinez E, Madrigal J, Vega JA, Gorostiaga P, Alexandrian D, Dimitrakopoulos A (2002) SAULTUS program – spot fires, knowledge and modelling. In 'Forest Fire Research and Wildland Fire Safety'. (Ed. DX Viegas) (CD-ROM) (Elsevier BV: Amsterdam, the Netherlands)

Colman JJ, Linn RR (2007) Separating combustion from pyrolysis in HIGRAD/FIRETEC. *International Journal of Wildland Fire* **16**, 493–502. doi:10.1071/WF06074

Crosby JS, Chandler CC (1966) Get the most from your windspeed observation. *Fire Control Notes* **27**(4), 12–13.

Cruz MG, Plucinski MP (2007) Billo Road Fire – report on fire behaviour phenomena and suppression activities. Bushfire Cooperative Research Centre, Report Number A.07.02. (Melbourne)

Cruz MG, Alexander ME, Wakimoto RH (2005) Development and testing of models for predicting crown fire rate of spread in conifer forest stands. *Canadian Journal of Forest Research* **35**, 1626–1639. doi:10.1139/X05-085

Cruz MG, Butler BW, Alexander ME, Forthofer JM, Wakimoto RH (2006) Predicting the ignition of crown fuels above a spreading surface fire. Part I. Model idealization. *International Journal of Wildland Fire* **15**, 47–60. doi:10.1071/WF04061

Cruz MG, Alexander ME, Fernandes PAM (2008) Development of a model system to predict wildfire behaviour in pine plantations. *Australian Forestry* **70**, 113–121.

Ellis PF (2000) The aerodynamic and combustion characteristics of eucalypt bark – a firebrand study. PhD thesis, Australian National University, Canberra, ACT.

Ellis PF (2011) Fuelbed ignition potential and bark morphology explain the notoriety of the eucalypt messmate 'stringybark' for intense spotting. *International Journal of Wildland Fire* **20**, 897–907. doi:10.1071/WF10052

Finklin AI (1973) Meteorological factors in the Sundance Fire run. USDA Forest Service, Intermountain Forest and Range Experiment Station, General Technical Report INT-6. (Ogden, UT)

Finney MA (2004) FARSITE: fire area simulator — model development and evaluation. USDA Forest Service, Rocky Mountain Research Station, Research Paper RMRS-RP-4 Revised. (Fort Collins, CO)

Forest Fire Management Group (2007) 'Softwood plantation fire synopsis.' (Primary Industry Ministerial Council, Forestry and Forest Products Committee: Canberra, ACT)

Fromm MD, Servranckx R (2003) Transport of forest fire smoke above the tropopause by supercell convection. *Geophysical Research Letters* **30**, 1542. doi:10.1029/2002GL016820

Fryer GI, Johnson EA (1988) Reconstruction of fire behaviour and effects in a subalpine forest. *Journal of Applied Ecology* **25**, 1063–1072. doi:10.2307/2403766

Ganteaume A, Lampin-Maillet C, Guijarro M, Hernando C, Jappiot M, Fonturbel T, Pérez-Gorostiaga P, Vega JA (2009) Spot fires: fuel bed flammability and capability of firebrands to ignite fuel beds. *International Journal of Wildland Fire* **18**, 951–969. doi:10.1071/WF07111

Gisborne HT (1927) Meteorological factors in the Quartz Creek forest fire. *Monthly Weather Review* **55**, 56–60. doi:10.1175/1520-0493(1927)55<56:MFITQC>2.0.CO;2

Gisborne HT (1935) Shaded fire breaks. *Journal of Forestry* **33**, 86–87.

Gisborne HT (1948) Fundamentals of fire behavior. *Fire Control Notes* **9**(1), 13–24.

Gostintisev YA, Sukhanov LA (1977) Convective column above a linear fire in a homogeneous isothermal atmosphere. *Fizika Goreniya I Vzryva* **13**, 675–685. [Translated into English in: *Physics of Combustion, Explosion, and Shock Waves* **13**, 570–579]

Gostintisev YA, Sukhanov LA (1978) Convective column above a linear fire in a polytropic atmosphere. *Fizika Goreniya I Vzryva* **14**, 3–8. [Translated into English in *Physics of Combustion, Explosion, and Shock Waves* **14**, 271–275]

Gould JS, McCaw WL, Cheney NP, Ellis PF, Knight IK, Sullivan AL (2007) 'Project Vesta. Fire in Dry Eucalypt Forest: Fuel Structure, Fuel Dynamics and Fire Behaviour.' (Ensis–CSIRO and Department of Environment and Conservation: Canberra, ACT and Perth, WA)

Grishin AM (1997) 'Mathematical Modeling of Forest Fires and New Methods of Fighting Them.' (Ed. F Albini) (Publishing House Tomsk State University: Tomsk, Russia) [Translated by M Czuma, L Chikina and L Smokotina]

Grishin AM, Gruzin AD, Vzerev VG (1981) Heat and mass transport and the propagation of burning particles in the surface layer of the atmosphere during upstream forest fires. *Fizika Gorenia i Vzryva* **17**, 78–84. [Translated into English in: *Physics of Combustion, Explosion, and Shock Waves* **17**, 418–423]

Haines DA, Smith MC (1987) Three types of horizontal vortices observed in wildland mass and crown fires. *Journal of Climate and Applied Meteorology* **26**, 1624–1637. doi:10.1175/1520-0450(1987)026<1624:TTOHVO>2.0.CO;2

Himoto K, Tanaka T (2005) Transport of disk-shaped firebrands in a turbulent boundary layer. In 'Eighth International Symposium on Fire Safety Science', 18–23 September 2005, Beijing, China. (Eds DT Gottuk, BY Lattimer) pp. 433–444. (International Association for Fire Safety Science: Baltimore, MD)

Hirsch SN, Meyer GF, Radloff DL (1979) Choosing an activity fuel treatment for Southwest ponderosa pine. USDA Forest Service, Rocky Mountain Forest and Range Experiment Station, General Technical Report RM-67. (Fort Collins, CO)

Jakeman AJ, Letcher RA, Norton JP (2006) Ten iterative steps in development and evaluation of environmental models. *Environmental Modelling & Software* **21**, 602–614. doi:10.1016/J.ENVSOFT.2006.01.004

Jemison GM (1932) Meteorological observations affecting the Freeman Lake (Idaho) Fire. *Monthly Weather Review* **60**, 1–2. doi:10.1175/1520-0493(1932)60<1:MCATFL>2.0.CO;2

Johansen RW (1981) Windrows vs small piles for forest debris disposal. *Fire Management Notes* **42**(1), 7–9.

Johnson VJ (1982) The dilemma of flame length and intensity. *Fire Management Notes* **43**(4), 3–7.

Johnson VJ (1984) How shape affects the burning of piled debris. *Fire Management Notes* **45**(3), 12–15.

Keeves A, Douglas DR (1983) Forest fires in South Australia on 16 February 1983 and consequent future forest management aims. *Australian Forestry* **46**, 148–162.

Kiil AD, Miyagawa RS, Quintilio D (1977) Calibration and performance of the Canadian Fire Weather Index in Alberta. Environment Canada, Canadian Forestry Service, Northern Forest Research Centre, Information Report NOR-X-173. (Edmonton, AB)

Koch E (1978) History of the 1910 forest fires in Idaho and western Montana. USDA Forest Service, Region 1. (Missoula, MT). In 'When the Mountains Roared: Stories of the 1910 Fire'. USDA Forest Service, Idaho Panhandle National Forests, Publication R1–78–30. (Coeur d'Alene, ID)

Koo E, Pagni PJ, Linn RR (2007) Using FIRETEC to describe firebrand behavior in wildfires. In 'The Tenth International Symposium of Fire and Materials', 29–31 January 2007, San Francisco, CA. (Interscience Communications: London, UK)

Koo E, Pagni PJ, Weise DR, Woycheese JP (2010) Firebrands and spotting ignition in large-scale fires. *International Journal of Wildland Fire* **19**, 818–843. doi:10.1071/WF07119

Lawson BD (1973) Fire behavior in lodgepole pine stands related to the Canadian Fire Weather Index. Canadian Forestry Service, Pacific Forest Research Centre, Information Report BC-X-176. (Victoria, BC)

Lawson BD, Armitage OB (2008) 'Weather Guide for the Canadian Forest Fire Danger Rating System.' (Natural Resources Canada, Canadian Forest Service, Northern Forestry Centre: Edmonton, AB)

Lee S-L (1972) Fire research. *Applied Mechanics Reviews* **25**, 503–509.

Lee S-L, Emmons HW (1961) A study of natural convection above a line fire. *Journal of Fluid Mechanics* **11**, 353–368. doi:10.1017/S0022112061000573

Lee S-L, Hellman JM (1970) Firebrand trajectory study using an empirical velocity-dependent burning law. *Combustion and Flame* **15**, 265–274. doi:10.1016/0010-2180(70)90006-4

Linn RR, Reisner J, Colman JJ, Winterkamp J (2002) Studying wildfire behavior using FIRETEC. *International Journal of Wildland Fire* **11**, 233–246. doi:10.1071/WF02007

List RJ (1951) 'Smithsonian Meteorological Tables', 6th rev. edn (Smithsonian Institution Press: Washington, DC)

Luke RH, McArthur AG (1978) 'Bushfires in Australia.' (Australian Government Publishing Service: Canberra, ACT)

Manzello SL, Cleary TG, Shields JR, Yang JC (2006) Ignition of mulch and grasses by firebrands in wildland–urban interface fires *International Journal of Wildland Fire* **15**, 427–431. doi:10.1071/WF06031

McArthur AG (1967) Fire behaviour in eucalypt forests. Commonwealth of Australia, Forestry and Timber Bureau, Forest Research Institute, Leaflet 100. (Canberra, ACT)

Mell WE, Jenkins MA, Gould JS, Cheney NP (2007) A physics-based approach to modelling grassland fires. *International Journal of Wildland Fire* **16**, 1–22. doi:10.1071/WF06002

Morris GA Jr (1987) A simple method for computing spotting distances from wind-driven surface fires. USDA Forest Service, Intermountain Research Station, Research Note INT-374. (Ogden UT)

Morton BR (1965) Modeling fire plumes. *Symposium (International) on Combustion* **10**, 973–982. doi:10.1071/WF06002

Nelson RM Jr (1980) Flame characteristics for fires in southern fuels. USDA Forest Service, Southeastern Forest Experiment Station, Research Paper SE-205. (Asheville, NC)

Noble IR, Bary GAV, Gill AM (1980) McArthur's fire-danger meters expressed as equations. *Australian Journal of Ecology* **5**, 201–203. doi:10.1111/J.1442-9993.1980.TB01243.X

Norum RA (1982) Predicting wildfire behavior in black spruce forests in Alaska. USDA Forest Service, Pacific Northwest Forest and Range Experiment Station, Research Note PNW-401. (Portland, OR)

O'Connor P, O'Connor B (1993) 'Out of the Ashes: the Ash Wednesday Bushfires in the South-east of SA, 16th February 1983.' (Millicent Press: Millicent, SA)

Partners in Protection (2003) 'FireSmart: Protecting your Community from Wildfire.' 2nd edn (Partners in Protection: Edmonton, AB)

Pastor E, Zárate L, Planas E, Arnaldos J (2003) Mathematical models and calculation systems for the study of wildland fire behavior. *Progress in Energy and Combustion Science* **29**, 139–153. doi:10.1016/S0360-1285(03)00017-0

Pisaric MFJ (2002) Long-distance transport of terrestrial plant material by convection resulting from forest fires. *Journal of Paleolimnology* **28**, 349–354. doi:10.1023/A:1021630017078

Potter BP (2011) Spot fires. In 'Synthesis of Knowledge of Extreme Fire Behavior: Volume 1 for Fire Managers'. USDA Forest Service, Pacific Northwest Research Station, General Technical Report PNW-GTR-854, pp. 81–87. (Portland, OR)

Quintilio D, Lawson BD, Walkinshaw S, Van Nest T (2001) Final documentation report – Chisholm Fire (LWF-063). Alberta Sustainable Resource Development, Forest Protection Division Report I/036. (Edmonton, AB)

Rice CL, Laing G, Gettle G (2010) New and novel ways to collect and characterize embers [abstract]. In 'Proceedings of 6th International Conference on Forest Fire Research', 15–18 November 2010, Coimbra, Portugal. (Ed. DX Viegas) (CD-ROM) (University of Coimbra: Coimbra, Portugal)

Roberts PJW (1979*a*) Line plume and ocean outfall dispersion. *Journal of the Hydraulics Division* **105**, 313–331.

Roberts PJW (1979*b*) Two-dimensional flow field of multiport diffuser. *Journal of the Hydraulics Division* **105**, 607–611.

Roberts PJW (1980) Ocean outfall dilution: effects of currents. *Journal of the Hydraulics Division* **106**, 769–782.

Rothermel RC (1968) Sundance Fire. *Fire Research Abstracts and Reviews* **10**, 127–129.

Rothermel RC (1983) How to predict the spread and intensity of forest and range fires. USDA Forest Service, Intermountain Forest and Range Experiment Station, General Technical Report INT-143. (Ogden, UT)

Rothermel RC (1991) Predicting behavior and size of crown fires in the Northern Rocky Mountains. USDA Forest Service, Intermountain Research Station, Research Paper INT-438. (Ogden, UT)

Rothermel RC (1993) Mann Gulch Fire: a race that couldn't be won. USDA Forest Service, Intermountain Research Station, General Technical Report INT-299. (Ogden, UT)

Rouse H, Yih CS, Humphreys HW (1952) Gravitational convection from a boundary source. *Tellus* **4**, 201–210. doi:10.1111/J.2153-3490.1952.TB01005.X

Roussopoulos PJ (1978) A decision aid for wilderness fire prescriptions in the Boundary Waters Canoe Area. In 'Preprint Volume of 5th National Conference on Fire and Forest Meteorology', 14–16 March 1978, Atlantic City, NJ. pp. 52–80. (American Meteorological Society: Boston, MA)

Sardoy N, Consalvi JL, Porterie B, Fernandez-Pello AC (2007) Modeling transport and combustion of firebrands from burning trees. *Combustion and Flame* **150**, 151–169. doi:10.1016/J.COMBUSTFLAME.2007.04.008

Sardoy N, Consalvi JL, Kaiss A, Fernandez-Pello AC, Porterie B (2008) Numerical study of ground-level distribution of firebrands generated by line fires. *Combustion and Flame* **154**, 478–488. doi:10.1016/J.COMBUSTFLAME.2008.05.006

Simard AJ, Haines DA, Blank RW, Frost JS (1983) The Mack Lake Fire. USDA Forest Service, North Central Forest Experiment Station, General Technical Report NC-83. (Saint Paul, MN)

Stocks BJ (1995) Fire behaviour and new fire development on escaped Carmody Township prescribed burn. In 'Prescribed Burn Program

Review – 1995'. Ontario Ministry of Natural Resources, Aviation, Flood and Fire Management, Appendix 4, pp. 1–4. (Sault Ste Marie, ON)

Stockstad DS (1979) Spontaneous and piloted ignition of rotten wood. USDA Forest Service, Intermountain Forest and Range Experiment Station, Research Note INT-267. (Ogden, UT)

Sullivan AL (2009) Wildland surface fire spread modeling, 1990–2007. 1. Physical and quasi-physical models. *International Journal of Wildland Fire* **18**, 349–368. doi:10.1071/WF06143

Sussot RA (1982) Characterization of the thermal properties of forest fuels by combustible gas analysis. *Forest Science* **28**, 404–420.

Sutton MW (1984) Extraordinary flame heights observed in pine fires on 16 February 1983. *Australian Forestry* **47**, 199–200.

Tarifa CS, del Notario PP, Moreno FG (1965) On the flight paths and lifetimes of burning particles of wood. Symposium (International) on Combustion 10, 1021–1037.

Taylor SW, Pike RG, Alexander ME (1997) Field guide to the Canadian Forest Fire Behavior Prediction (FBP) System. Natural Resources Canada, Canadian Forest Service, Northern Forestry Centre, Special Publication 11. (Edmonton, AB)

Thomas PH (1965) A comparison of some hot-spot theories. *Combustion and Flame* **9**, 369–372. doi:10.1016/0010-2180(65)90025-8

Thomas PH (1973) An approximate theory of 'hot spot' criticality. *Combustion and Flame* **21**, 99–109. doi:10.1016/0010-2180(73)90011-4

Tinner W, Hofstetter S, Zeugin F, Conedera M, Wohlgemuth T, Zimmerman L, Zweifel R (2006) Long-distance transport of macroscopic charcoal by an intensive crown fire in the Swiss Alps – implications for fire history reconstruction. *The Holocene* **16**, 287–292. doi:10.1191/0959683606HL925RR

USDA Forest Service (1952) Fire studies. In 'Annual Report – 1951'. USDA Forest Service, Pacific Northwest Forest and Range Experiment Station, pp. 41–43. (Portland, OR)

USDA Forest Service (1960) Ember-lifting power of convection column updrafts. In 'Annual Report, 1959'. USDA Forest Service, Southeastern Forest Experiment Station, pp. 42–43. (Asheville, NC)

Van Wagner CE (1977) Conditions for the start and spread of crown fire. *Canadian Journal of Forest Research* **7**, 23–34. doi:10.1139/X77-004

Venkatesh S, Saito K, Rothermel RC (2000) Maximum spotting distance in wind-driven crown fires. *Nensho no Kagaku to Gijutsu* **7**, 221–233 [In English]

Wade DD, Ward DE (1973) An analysis of the Air Force Bomb Range Fire. USDA Forest Service, Southeastern Forest Experiment Station, Research Paper SE-105. (Asheville, NC)

Wang HH (2011) Analysis of downwind distribution of firebrands sourced from a wildland fire. *Fire Technology* **47**, 321–340. doi:10.1007/S10694-009-0134-4

Watts JM Jr (1987) Editorial: validating fire models. *Fire Technology* **23**, 93–94. doi:10.1007/BF01040425

Weir JR (2004) Probability of spot fires during prescribed burns. *Fire Management Today* **64**(2), 24–26.

Weir JR (2009) 'Conducting Prescribed Fires: a Comprehensive Manual.' (Texas A&M University Press: College Station, TX)